Plant Biotechnology Journal
Open Access

Plant Biotechnology Journal (2023), pp. 1–17 doi: 10.1111/pbi.14025

TaTPP-7A positively feedback regulates grain filling and wheat grain yield through T6P-SnRK1 signalling pathway and sugar–ABA interaction

Hongxia Liu[1,*], Xuemei Si[1], Zhenyu Wang[1], Liangjing Cao[1], Lifeng Gao[1], Xiaolong Zhou[2], Wenxi Wang[3], Ke Wang[1], Chengzhi Jiao[1], Lei Zhuang[1], Yunchuan Liu[1], Jian Hou[1], Tian Li[1], Chenyang Hao[1], Weilong Guo[3], Jun Liu[1] and Xueyong Zhang[1,*]

[1]*National Key Facility for Crop Gene Resources and Genetic Improvement, Institute of Crop Sciences, Chinese Academy of Agricultural Sciences (CAAS), Beijing, China*
[2]*Beijing Biomics Biotechnology Company limited, Beijing, China*
[3]*Frontiers Science Center for Molecular Design Breeding, China Agricultural University, Beijing, China*

Received 29 September 2022;
revised 26 January 2023;
accepted 30 January 2023.
**Correspondence* (Tel +86 1082105826; fax +86 1082106695; email liuhongxia02@caas.cn (H. X. L.);
Tel +86 1082105826;
fax +86 1082106695;
email zhangxueyong@caas.cn (X. Y. Z.))

Keywords: wheat, yield, grain filling, T6P, sucrose feedback regulation, ABA.

Summary

Grain size and filling are two key determinants of grain thousand-kernel weight (TKW) and crop yield, therefore they have undergone strong selection since cereal was domesticated. Genetic dissection of the two traits will improve yield potential in crops. A quantitative trait locus significantly associated with wheat grain TKW was detected on chromosome 7AS flanked by a simple sequence repeat marker of *Wmc17* in Chinese wheat 262 mini-core collection by genome-wide association study. Combined with the bulked segregant RNA-sequencing (BSR-seq) analysis of an F_2 genetic segregation population with extremely different TKW traits, a candidate trehalose-6-phosphate phosphatase gene located at 135.0 Mb (CS V1.0), designated as *TaTPP-7A*, was identified. This gene was specifically expressed in developing grains and strongly influenced grain filling and size. Overexpression (OE) of *TaTPP-7A* in wheat enhanced grain TKW and wheat yield greatly. Detailed analysis revealed that OE of *TaTPP-7A* significantly increased the expression levels of starch synthesis- and senescence-related genes involved in abscisic acid (ABA) and ethylene pathways. Moreover, most of the sucrose metabolism and starch regulation-related genes were potentially regulated by SnRK1. In addition, *TaTPP-7A* is a crucial domestication- and breeding-targeted gene and it feedback regulates sucrose lysis, flux, and utilization in the grain endosperm mainly through the T6P-SnRK1 pathway and sugar–ABA interaction. Thus, we confirmed the T6P signalling pathway as the central regulatory system for sucrose allocation and source–sink interactions in wheat grains and propose that the trehalose pathway components have great potential to increase yields in cereal crops.

Introduction

Bread wheat (*Triticum aestivum* L.) is the most important staple food in the world that provides approximately 20% of calories for the global population (Pfeifer *et al*., 2014). In China, wheat holds the third position in crop productivity and contributes about 130 million tonnes of grain per year (http://www.fao.org/worldfoodsituation/csdb/en/). However, the world population is expected to reach approximately 9 billion by 2050, and it demands at least a 50% increase in the production of major crops (Godfray *et al*., 2010), including wheat, rice (*Oryza sativa* L.), and maize (*Zea mays* L.). Therefore, there is an urgent need to discover novel key genes and elucidate the complicated molecular mechanisms of sustainably improving yield for developing high-yielding and widely adapted wheat varieties.

In wheat, yield depends primarily on spike number per unit area, grain number per spike, and thousand kernel weight (TKW) (Xiao and He, 2003). Among these, TKW is the most stable and heritable characteristic (Xiao and He, 2003) and is mainly determined by grain size (volume) and grain filling (plumpness) (Sakamoto and Matsuoka, 2008). Grain size is characterized by a combination of grain length (GL), grain width (GW), grain thickness (GT), and grain length-to-width ratio, which positively affects yield (Zuo and Li, 2014). In rice, more than 400 quantitative trait loci (QTLs) associated with grain traits have been identified, and dozens of related genes, such as *Dwarf1* (Ashikari *et al*., 1999), *GS3* (Fan *et al*., 2006), *GW2* (Song *et al*., 2007), *GW5* (Weng *et al*., 2008), *GS5* (Li *et al*., 2011), *GW8* (Wang *et al*., 2012b), and *GIF1* (Wang *et al*., 2008), have been cloned. These genes mainly regulate cell division, proliferation, and elongation and are involved in multiple signalling pathways, such as ubiquitination-mediated proteasomal degradation, G protein signalling, MAPK signalling, and phytohormone signalling (Zuo and Li, 2014), indicating a complex mechanism regulating grain size in crops. However, studies on the molecular cloning of genes associated with grain weight in wheat are limited. Currently, only 15 genes, including *TaGW2* (6A, 240.3 Mb; Su *et al*., 2011), *TaGS5-3A* (3A, 188.2 Mb; Ma *et al*., 2016),

Please cite this article as: Liu, H., Si, X., Wang, Z., Cao, L., Gao, L., Zhou, X., Wang, W., Wang, K., Jiao, C., Zhuang, L., Liu, Y., Hou, J., Li, T., Hao, C., Guo, W., Liu, J. and Zhang, X. (2023) *TaTPP-7A* positively feedback regulates grain filling and wheat grain yield through T6P-SnRK1 signalling pathway and sugar–ABA interaction. *Plant Biotechnol J*., https://doi.org/10.1111/pbi.14025.

© 2023 The Authors. *Plant Biotechnology Journal* published by Society for Experimental Biology and The Association of Applied Biologists and John Wiley & Sons Ltd.
This is an open access article under the terms of the Creative Commons Attribution-NonCommercial-NoDerivs License, which permits use and distribution in any medium, provided the original work is properly cited, the use is non-commercial and no modifications or adaptations are made.

14677652, 0, Downloaded from https://onlinelibrary.wiley.com/doi/10.1111/pbi.14025 by Chinese Academy Of, Wiley Online Library on [15/03/2023]. See the Terms and Conditions (https://onlinelibrary.wiley.com/terms-and-conditions) on Wiley Online Library for rules of use; OA articles are governed by the applicable Creative Commons License

TaCKX6-D1 (3D, 106.2 Mb; Zhang *et al*., 2012), *TaGASR7* (7A, 176.0 Mb; Zhang *et al*., 2015a), *TaTGW-7A* (7A, 211.6 Mb; Hu *et al*., 2016), *TaGW8* (7A, 257.3 Mb; Yan *et al*., 2019), *TaGW7* (2A, 139.7 Mb; Wang *et al*., 2019a), *TaDA1* (2A, 8.3 Mb; Liu *et al*., 2020), and *TaIAA21* (7A, 488.5 Mb; Jia *et al*., 2021), have been reported to contribute to grain size and/or weight in wheat. Research has also indicated that the mechanism regulating grain size is conserved across cereal crops (Zuo and Li, 2014); however, the mechanism underlying an increase in grain yield, especially grain filling, in rice, wheat, and other cereal crops remains elusive.

Grain filling is a complex process that involves the remobilization of photoassimilates, mainly sucrose, to the developing grains, where sucrose is converted to starch through a series of enzymatic reactions. In wheat endosperm, starch content accounts for 65%–80% of the mature grains; therefore, grain filling is a crucial determinant of wheat yield. Besides, sucrose, the primary photosynthetic product that moves a long distance from green leaves to various sink organs via the phloem, is the substrate of starch synthesis and therefore plays a vital role in determining grain TKW and wheat yield (Figueroa and Lunn, 2016; Hou *et al*., 2014); however, the specific molecular mechanism regulating sucrose unloading and metabolism in grains remains largely unknown. Therefore, finding the key regulator of sucrose metabolism will help for the regulation of yield improvement in wheat. In recent years, trehalose (Tre) metabolism components, especially trehalose-6-phosphate (T6P), have gained much research attention due to their roles in regulating plant growth and development, as well as the newly identified potential role of T6P in regulating yield in major cereal crops (Nuccio *et al*., 2015; Paul *et al*., 2020; Zhang *et al*., 2017). In higher plants, Tre and T6P, which exist in trace amounts, are formed mainly via a two-step pathway and serve as energy sources and signalling components (Paul, 2008; Schluepmann *et al*., 2003). First, T6P is formed from UDP-glucose and glucose-6-phosphate (G6P) under the action of trehalose-6-phosphate synthase (TPS). Subsequently, trehalose-6-phosphate phosphatase (TPP) dephosphorylates T6P to Tre. However, studies have indicated that T6P is more important than Tre as a sugar signal in plants, which acts as a key and specific signal for sucrose abundance and carbon availability (O'Hara *et al*., 2013; Paul, 2008; Schluepmann *et al*., 2003). T6P has been implicated in sucrose and starch regulation in *Arabidopsis thaliana* leaves (Lunn *et al*., 2006; Schluepmann and Paul, 2009) and wheat grains (Martínez-Barajas *et al*., 2011). In addition, several studies have highlighted the central role of T6P in regulating crop productivity. A *RAMOSA3* (*RA3*) gene encoding a TPP protein in maize determines inflorescence architecture (Satoh-Nagasawa *et al*., 2006). In addition, overexpression (OE) of a rice *TPP* gene in the developing maize ear increased kernel set and harvest index and improved yield under drought conditions (Nuccio *et al*., 2015). Meanwhile, in wheat, changes in the single nucleotide polymorphism (SNP) in the *TaTPP-6AL* genome have been correlated with yield (Zhang *et al*., 2017). However, the exact molecular basis of T6P-mediated regulation of sucrose level, sugar flow from T6P to starch synthesis, and eventually yield improvement remains unclear yet.

In the present study, we used a genome-wide association study (GWAS) in Chinese 262 mini-core collection (MCC) combined with bulked segregant RNA-sequencing (BSR-seq) analysis in an F_2 biparental progeny with extremely different TKW traits to identify the key genes associated with TKW and regulating sucrose metabolism in wheat grain. We detected a gene, *TaTPP-7A* (*Triticum aestivum* trehalose-6-phosphate phosphatase), on chromosome 7AS significantly associated with grain TKW and found it as a member of HAD superfamily IIB subfamily of the Tre pathway. OE of *TaTPP-7A* in wheat resulted in higher TKW, longer grains, and quicker grain filling, whereas the *TaTPP-7A* RNAi lines or gene-edited mutants displayed lower TKW, shorter grains, and slower filling. Results demonstrated that *TaTPP-7A* feedback regulates sucrose lysis, flux, and utilization in the grain endosperm and consequently affects grain filling and yield mainly through the T6P-SnRK1 (sucrose non-fermenting (SNF1)-related protein kinase 1) pathway and sugar–ABA interaction. The work highlights the importance of the T6P signalling pathway, and established it as the central regulatory system for sucrose allocation and source–sink interactions in wheat grains and proposes *TaTPP-7A* and Tre pathway components as candidates for improving grain size and yield in wheat.

Results

Identification of *TaTPP-7A* by GWAS combined with BSR-seq

Chinese 262 MCC, representing more than 70% of the diversity in Chinese wheat and with highly heritable, domesticated traits, have been proven to be a suitable natural population for primary QTL mapping or gene identification in wheat (Wang *et al*., 2012a). In the present study, a QTL significantly associated with TKW was identified on Chr.7AS ($-\log_{10}P > 4.07$) under four environments by GWAS among 262 MCC (Figure 1a). During 2005–2006, this locus was anchored by four peak SNPs closely clustered within a 339 bp distance (Table S1). The associated physical distance of the peaked SNPs ($-\log_{10}P > 4.38$, at 127.76 (CS V1.0)/131.21 (CS V2.1) Mb) was estimated as 8.88 Mb when r^2 of the linkage disequilibrium (LD) decayed to 0.2 (Figure 1b). Therefore, we choose the 9.0 Mb physical distance (at 127–136 Mb, CS V1.0) as the candidate region to identify the associated candidate genes. We found that a simple sequence repeat (SSR) marker of *Wmc17*, previously reported significantly associated with TKW among 262 MCC under four environments by Wang *et al*. (2012a), falls within this reasonable LD attenuation range and has a physical distance of about 7.4 Mb to the peaked GWAS loci. Compared with the other unfavoured alleles, the favoured allele of the *Wmc17* marker showed a mean TKW difference of 5.32 g ($P < 0.001$) and explained more than 19.62% of the total phenotypic variation (Wang *et al*., 2012a). In addition, as an SSR marker, we further proved that *Wmc17* was only located on the short arm of Chr.7A at 135.0/138.61 Mb (CS V1.0/2.1) (Figures S1, S2 and Table S2). Thus, we assumed that one major TKW-associated candidate gene was located near or within this GWAS loci.

To further solidify the above speculation and identify the candidate genes, an F_2 segregation population with a mean TKW difference of 35.37 g between the two parents was developed (Figure 1c, Figure S3), followed by BSR-seq analysis in developing grains to identify the candidate differentially expressed genes (DEGs) in the associated interval (127–136/131–140 Mb for Chines spring (CS) V1.0/V2.1, respectively) using two bulks with extremely different TKW. Totally, we identified 10 149 DEGs from the two parents (PH/PL) and the two bulks. Among them, 9276 DEGs were detected between PH and PL and 1255 between the two bulks. The KEGG pathway enrichment analysis using all the DEGs highlighted the starch and sucrose metabolism pathway ($P < 0.0001$), which was the most predominant both in parents

© 2023 The Authors. *Plant Biotechnology Journal* published by Society for Experimental Biology and The Association of Applied Biologists and John Wiley & Sons Ltd.,

14677652, 0, Downloaded from https://onlinelibrary.wiley.com/doi/10.1111/pbi.14025 by Chinese Academy Of, Wiley Online Library on [15/03/2023]. See the Terms and Conditions (https://onlinelibrary.wiley.com/terms-and-conditions) on Wiley Online Library for rules of use; OA articles are governed by the applicable Creative Commons License

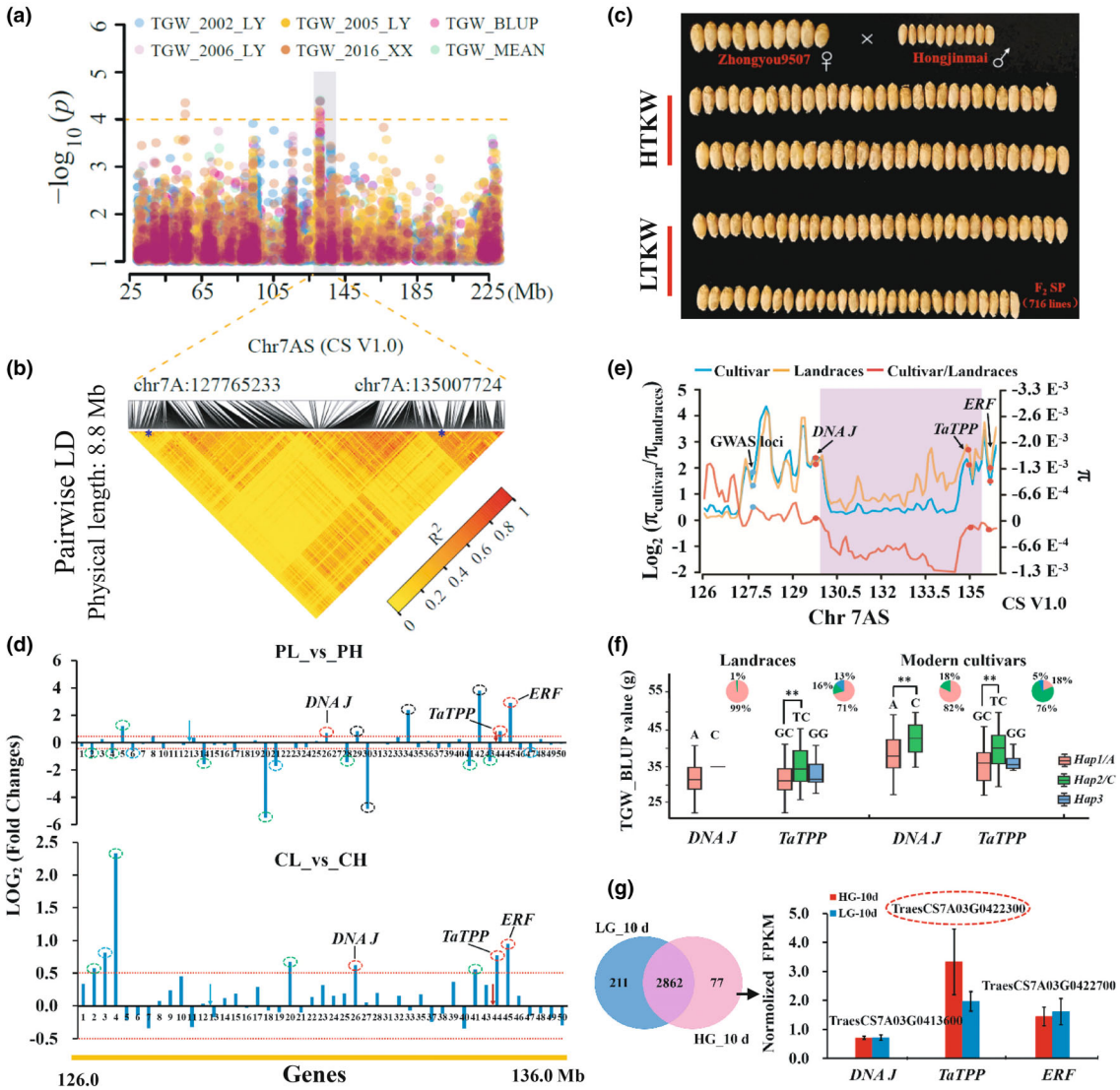

Figure 1 Mapping and identification of *TaTPP-7A* (a) Manhattan plot shows the genome-wide loci significantly associated with TKW in the 25–225 Mb region on chromosome 7AS. The dashed yellow line indicates the significance threshold ($-\log_{10}P = 4.0$). Shading indicates the estimated LD decay distance of the peaked SNPs. (b) Heatmap of LD for the peaked SNPs within 10 Mb. Blue asterisks indicate the significant SNPs and the *Wmc17* SSR marker. (c) Mature grains of the two parents and the F_2 segregation progeny used for BSR-seq. Zhongyou9507, maternal parent (MTKW = 60.2 g); Hongjinmai, paternal parent (MTKW = 24.8 g); HTKW and LTKW denote high and low TKW grains, respectively. (d) A comparison of the expression differences in the DEGs calculated from two parents (PL_PH) and two bulks (CL_CH) used for BSR-seq. DEGs in the 126–136 Mb region of chromosome 7AS are shown. The red dashed line indicates the threshold of $\log_2$ (FC) ≥ 0.5. The oval circles in different colours indicate the genes with no expression (black circle), no significant expression difference (blue circle), and different expression patterns (green circle) in any group or both groups; red circles represent the candidate DEGs. Red and blue arrows denote the physical loci of the SSR marker and the genome-wide significant loci, respectively. (e) Nucleotide diversity (π) and breeding sweep (red lines) of the landraces (157, orange lines) and modern cultivars (105, blue lines) within the 126–136 Mb interval on Chr.7AS. Purple shading indicates the breeding sweep under the horizontal threshold line. Blue and red dots denote genome-wide significant loci and candidate genes, respectively. (f) Haplotype plot verifies variations in the three candidate genes in 262 MCC. Accessions were classified based on the SNPs (A vs. C for *DNAJ*) or haplotypes (GC, TC vs. GG for *TaTPP-7A*). Pie charts (above) show the percentage of the two SNPs or three haplotypes. ** Denotes statistically significant differences between SNPs or haplotypes at $P < 0.01$ level. (g) Verification of the candidate gene expressions in the developing wheat grains at 10 DPA by RNA-seq. The blue/pink circle shows the Venn diagram of DEGs. HG and LG denote grains with higher and lower TKW, respectively. The histogram was plotted based on the normalized FPKM values for each candidate gene.

(177/3346) and bulks (47/464) among the top 20 enriched pathways (Figure S4).

The analysis of the expression pattern of the DEGs among the parent pool and the bulks identified only three DEGs (red circle), with a significant expression difference and the same expression trend, as candidates in the associated genomic interval (Figure 1d). Gene annotation showed that the first candidate *TraesCS7A03G0413600* encodes a mitochondrial chaperone protein DNA J1 in *Arabidopsis*, which is uncharacterized in wheat; genotyping showed no SNP variation in this gene within the landraces (Figure 1f). The second candidate *TraesCS7A03G0422300* (*TaTPP-7A*) encodes a *TPP* in rice and wheat

© 2023 The Authors. *Plant Biotechnology Journal* published by Society for Experimental Biology and The Association of Applied Biologists and John Wiley & Sons Ltd., 1–17

14677652, 0, Downloaded from https://onlinelibrary.wiley.com/doi/10.1111/pbi.14025 by Chinese Academy Of, Wiley Online Library on [15/03/2023]. See the Terms and Conditions (https://onlinelibrary.wiley.com/terms-and-conditions) on Wiley Online Library for rules of use; OA articles are governed by the applicable Creative Commons License

and is involved in carbohydrate transport and metabolism pathway (GO: 0005975); genotyping showed that this gene formed three haplotypes in the Chinese landraces and modern cultivars and was significantly associated with TKW under four environments (Figure 1f). In 2005, the differences in TKW between the highest (*Haplotype 1* (*Hap 1*)) and the lowest (*Hap 2*) *TaTPP-7A haps* were about 4.26 and 4.74 g for the landraces and the modern cultivars, respectively ($P < 0.001$). The third candidate *TraesCS7A03G0422700* encodes an AP_2 domain-containing ethylene-responsive transcription factor (*ERF*) in *Arabidopsis* and is uncharacterized in wheat; genotyping showed no SNP variation of this gene in the 262 MCC. Moreover, among the three candidate genes, the π of *TraesCS7A03G0422300* (*TaTPP-7A*) was much higher in landraces than in modern cultivars and fell within the breeding selection sweep in this interval (Figure 1e). Thus, we assumed *TaTPP* as the likely candidate.

For further confirmation, we analysed the expression patterns of the three candidate genes by RNA-seq in the developing grains (10 days postanthesis (DPA), derived from F_2 segregation progeny) with a mean TKW difference of 3.12–4.25 g between the high-TKW and the low-TKW ones. As shown in Figure 1g, only *TaTPP-7A* showed a high expression difference between these two sets of grains ($P < 0.05$), consistent with the BSR-seq data (Figure S5). Digital gene expression transcriptome data obtained from different tissues or different developmental stage grains of CS confirmed that *TaTPP-7A* is the only gene specifically expressed in wheat grains compared with the other genes located within the 2 Mb region (134.0–136.0/137.61–139.61 Mb for CS V1.0/V2.1, respectively) near the *Wmc17* (Figure S6). These observations confirmed *TaTPP-7A* as the TKW-associated candidate gene in this interval and were used for further confirmation by transgenic experiments.

TaTPP-7A encodes a functional T6P dephosphorylation enzyme of the Tre pathway and is highly expressed in the aleurone layer of the developing grains

Analysis of the predicted protein sequences revealed that TaTPP-7A and its homoeologs TaTPP-7B/7D are members of the IIB subfamily of HAD superfamily (http://www.ebi.ac.uk/InterProScan/), with the conserved TPP domains (Figure 2a). The genomic structures of the three homoeologous *TaTPP-7A/7B/7D*, were all comprised of ten exons and nine introns with the genomic sequence length of 2162, 2181 and 2118 bp, respectively. Full-length cDNA sequences of *TaTPP-7A/7B/7D* were 1083, 1092, and 1089 bp, respectively, which encoded 361, 364, and 363 amino acids (aa) (Figure 2b). The alignment of the TaTPP-7A/7B/7D protein sequences showed a high 97.53% similarity among them, with a 100% similarity for the four enzyme active sites, motifs I (DYDGTL, 110–115), II (TG, 148–149), III (K, 270), and IV (GD-nDh, 295–296 and 300), indicating a conserved and redundant function among the three homoeologs (Figure 2a). The phylogenetic tree constructed using the TPP proteins of various species presented wheat in a specific branch for cereals with rice and maize (Figure 2c) together and separated from the adjacent *Arabidopsis* clade (AtTPPJ and AtTPPI), indicating a new role of *TaTPPs* in cereals. Further expression analysis of the three homoeologous genes showed high and specific expression of *TaTPPs* in the young spikes and the developing grains (Figure 2d). The transcript level of *TaTPPs* in the grain tissues increased towards the filling stage (10–15 DPA), with at least three times higher expression than in the other tissues and developmental stages. Digital expression transcriptome data of CS showed that *TaTPPs* were specifically expressed in the aleurone layer of grains, and the expression abundance of *TaTPP-7A* at the filling stage (10–20 DPA) was much higher than the other two homoeologous genes (Figure S7), validating our results. Further, we found that the expression level of *TaTPPs* in the high TKW varieties with *Hap I* was 2–3 times higher than in the low TKW varieties with *Hap II* (Figure 2e), indicating *TaTPP-7A* as a TKW-associated, functional gene positively related to grain filling in wheat.

TaTPP-7A promotes grain development and filling, resulting in higher TKW and early maturity

Subsequent transgenic experiments showed that the OE of *TaTPP-7A* in wheat resulted in stable and significantly greater TKW ($P < 0.01$), longer GL ($P < 0.01$ or $P < 0.05$), and quicker filling ($P < 0.01$) compared with the WT and RNAi transformants (Figure 3a–d); however, other traits such as plant height (PH), spikelet number (SLN), spike number per plant (SN), and grain number (GN) showed no difference in three environments (Figures S8a and S9). The OE lines showed maximal 11.5 g higher TKW and 0.33 mm longer grains than the wide-type (WT), while the RNAi lines had 6.9 g lower TKW and 0.32 mm shorter grains. Yield per plant and estimated grain yield of the transgenic OE lines were enhanced by 24% while the RNAi lines declined by 20.4% compared with those of WT in 2017 (Figure S8b; $P < 0.01$). In addition, grain filling in the OE lines started 2–5 days earlier than in the WT and RNAi ones; the peak filling rate in the OE lines was 10.58% and 35.29% higher than in the WT and RNAi lines, respectively (Figure 3d). Huge differences were detected in TKW and other traits ($P < 0.05$ and $P < 0.01$) of the developing grains of the transgenic lines as early as 5 DPA (Figure 3c, Figure S10), with a good linear correlation ($R^2 = 1$) between filling rate and the expression level of *TaTPP-7A* in these transgenic lines (Figure 3d). Furthermore, the size changes in the lemma and palea of the transgenic lines confirmed the role of *TaTPP-7A* in regulating TKW; the OE of *TaTPP-7A* led to wider lemma and palea compared with the WT ($P < 0.01$; Figure S11), while RNAi resulted in shorter lemma and palea ($P < 0.01$). Meanwhile, *CriTaTPPs* (Figure S12) showed a significant 82%, 44.8%, and 28% decrease in GN, SLN, and spike length (SL), respectively, compared with the WT ($P < 0.01$; Figure 3e–g). Similarly, the *K-TaTPPs* also exhibited a significant decrease in grain size, GN, and yield (Figure 3h, Figure S13). These observations suggested that *TaTPP-7A* is the TKW-associated gene within the GWAS loci and positively regulates grain filling in wheat.

TaTPP-7A affects endosperm amylose content, influencing starch gelatinization temperature and processing quality

Subsequently, to verify the molecular mechanism of *TaTPP-7A* regulating TKW or grain filling in wheat, we evaluated the total starch and amylose content in these transgenic lines and analysed the starch granules in the grain endosperm. Results showed that the OE of *TaTPP-7A* led to lower amylose content and amylose/amylopectin ratio compared with the WT ($P < 0.05$), but with no statistically significant difference in the total starch content though it increased by 2.53% compared to WT (Figure 4a). The OE lines had more number of spherical A-type starch granules ($P < 0.05$), which were arranged regularly and packed densely (Figure 4b), compared with those in WT and RNAi lines. While in the RNAi lines, the starch granules were arranged irregularly and stacked loosely; these lines had three times more A-type starch

© 2023 The Authors. *Plant Biotechnology Journal* published by Society for Experimental Biology and The Association of Applied Biologists and John Wiley & Sons Ltd.,

14677652, 0, Downloaded from https://onlinelibrary.wiley.com/doi/10.1111/pbi.14025 by Chinese Academy Of, Wiley Online Library on [15/03/2023]. See the Terms and Conditions (https://onlinelibrary.wiley.com/terms-and-conditions) on Wiley Online Library for rules of use; OA articles are governed by the applicable Creative Commons License

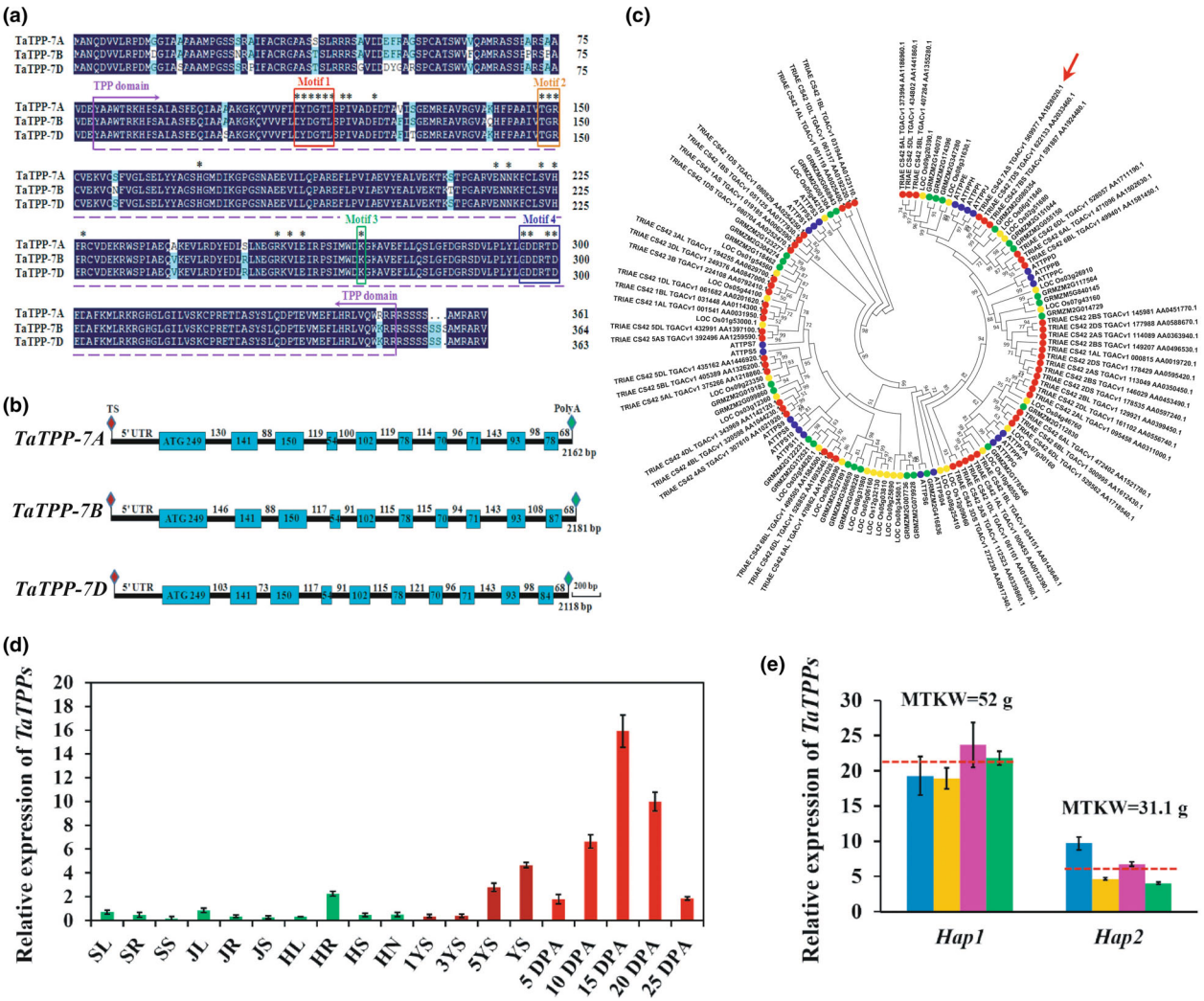

Figure 2 Sequence analysis and expression characteristics of *TaTPPs* (a) Deduced amino acid sequences of the three homoeologs of *TaTPPs*. Coloured boxes indicate different protein motifs, an asterisk corresponds to the enzyme active site, and purple arrows and dashed lines represent the predicted phosphatase domains (Swiss-Prot). (b) Genomic structure of three homoeologs of *TaTPPs*. Boxes correspond to exons. Dashes between the exons correspond to introns. Numbers correspond to the base number. (c) Phylogenetic relationships of HAD superfamily proteins with TPP domains in various plant species. Proteins with sequences matching the TPP homologous domain were retrieved from the Ensemble Plants public database. Blue, yellow, green, and red denote proteins from *Arabidopsis thaliana*, rice, maize, and wheat. The phylogenetic tree was constructed following the neighbour-joining method based on 1000 bootstrap replicates in MEGA7.0. (d) Expression patterns of *TaTPPs* in CS at various developmental stages and different tissues analysed by qRT-PCR. SL, SR, and SS indicate the leaves, roots, and stems of the seedlings; JL, JR, JS, HL, HR, HS, and HN indicate the leaves (L), roots (R), stem (S), and nodes (N) at jointing (J) and heading (H) stages; 1/3/5 YS and YS indicate young spikes 1/3/5 cm and 5–10 cm long; DPA indicates days postanthesis. Actin was used as the internal control. Bars indicate the standard error. (e) Expression analysis of *TaTPPs* in different wheat varieties with different haplotypes by qRT-PCR. *Hap I/II* represents the highest/lowest TKW haplotypes. MTKW denotes the average TKW of each *Hap* category.

granules, which appeared distorted with an obvious surface sunk ($P < 0.05$) compared with those in the OE lines and WT. Meanwhile, both single and double mutants of *CriTaTPPs* had flat and smaller grains and showed a decrease in the total number and diameter of the starch granules ($P < 0.001$; Figure 4c,f), with an apparent large cavity in the endosperm. However, the total granule number difference reached statistically significant levels only in the 7A/*7b*/*7d* double mutants compared with the WT, indicating a more substantial effect of *TaTPP-7A* on grain filling than GN.

Furthermore, we analysed the physicochemical properties, including thermal and pasting properties, of starches in the transgenic lines to investigate the effect of the increase in grain size and the decrease in amylose content on the starch processing qualities (Figure 4d,e, Table S3). The OE lines had significantly lower thermal and pasting parameters, including the peak onset (To), maximum (Tp), and conclusion (Tc) temperature, peak area (enthalpy, ΔH), trough viscosity (TV), final viscosity (FV), pasting peak time (TPV), and the average chain length, than the WT and RNAi lines ($P < 0.05$); however, the RNAi lines showed the lowest pasting temperature (PT), the highest peak viscosity (PV), and delayed TPV onset; the other thermal parameters and the average chain length showed no remarkable differences between WT and RNAi lines, indicating the role of *TaTPP-7A* in inducing changes in starch PT and physicochemical properties, which profoundly influenced wheat quality.

© 2023 The Authors. *Plant Biotechnology Journal* published by Society for Experimental Biology and The Association of Applied Biologists and John Wiley & Sons Ltd., 1–17

14677652, 0, Downloaded from https://onlinelibrary.wiley.com/doi/10.1111/pbi.14025 by Chinese Academy Of, Wiley Online Library on [15/03/2023]. See the Terms and Conditions (https://onlinelibrary.wiley.com/terms-and-conditions) on Wiley Online Library for rules of use; OA articles are governed by the applicable Creative Commons License

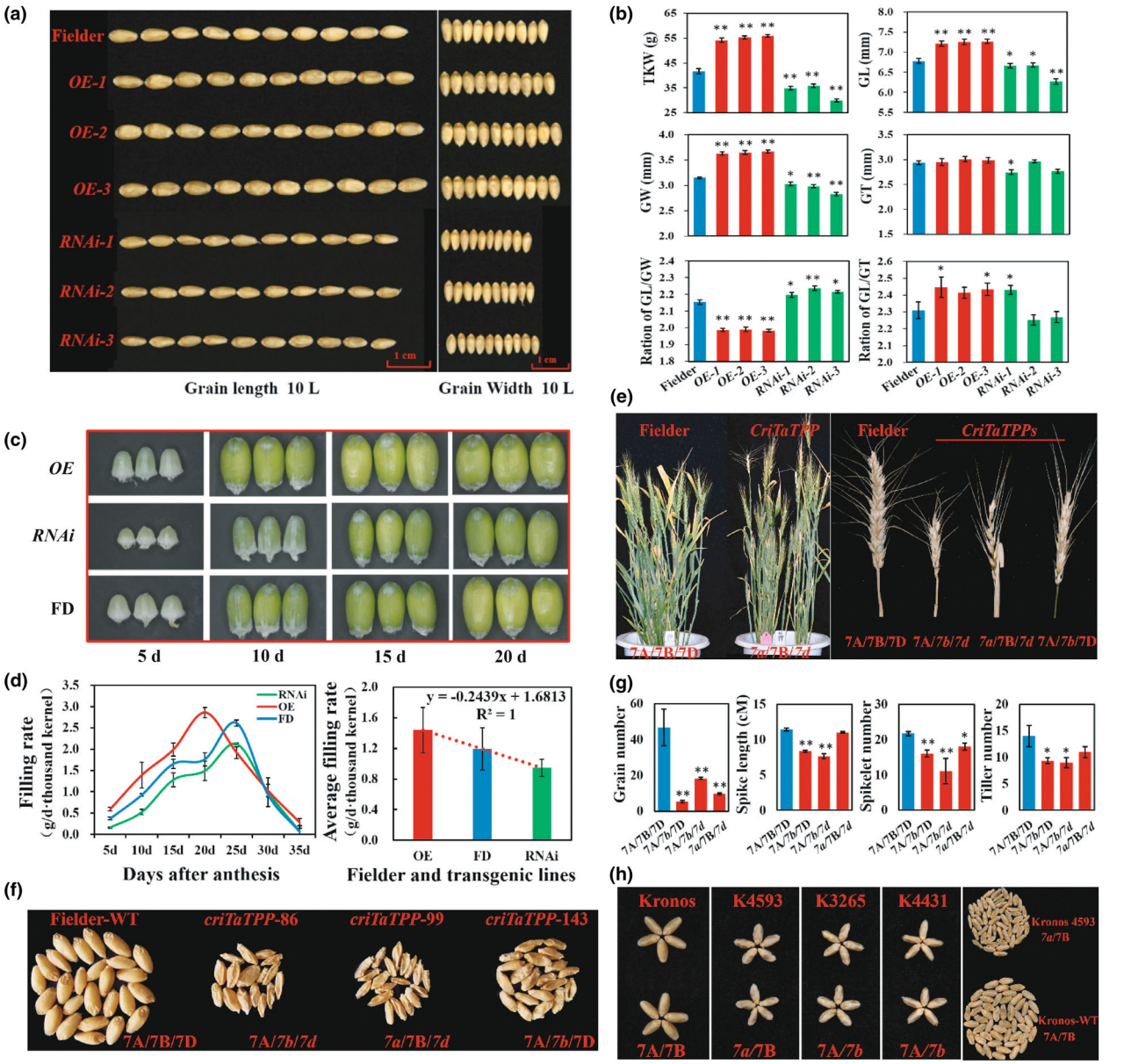

Figure 3 Grain phenotype and agronomic traits of transgenic *TaTPP-7A* lines (a) Mature grains of *TaTPP-7A* OE and RNAi wheat lines and the WT cv. Fielder. The grains show differences in length and width. Bar = 1 cm. (b) Grain traits of *TaTPP-7A* OE wheat lines and Fielder. TKW, thousand kernel weight; GL, grain length; GW, grain width; GT, grain thick; GL/GW, GL/GT, or GW/GT, the ratio of GL to GW, GL to GT, or GW to GT, respectively. (c) Developing grain phenotype. (d) Grain filling rate. R^2 and dashed red lines denote the correlation coefficient and the association between filling rate and transgenic lines, respectively. Bars show the standard error. (e, f, g) Phenotypes (whole plant, spike, and grain) and agronomic traits of *CriTaTPPs* mutants. *CriTaTPPs* denote the CRISPR/Cas9-edited lines of *TaTPPs*. Capital letters (7A/7B/7D) or italic lowercase letters (*7a/7b/7d*) denote the WT and mutant chromosomes. (h) Mature grains of the *K-TaTPP-7A/7B* mutants.

TaTPP-7A enhances starch synthesis and grain filling mainly through T6P-SnRK1 pathway and sugar–ABA interaction

Transcriptome sequencing was performed to elucidate the molecular mechanism of *TaTPP-7A* regulating starch synthesis. Totally, 11 339 DEGs were found commonly expressed among the OE, RNAi lines, and WT plants, while 1479 and 661 were specifically expressed in the OE and RNAi lines compared to WT plants (Figure 5a). KEGG pathway analysis of all these DEGs highlighted an enrichment of carbohydrate metabolism and transportation pathways, such as carbohydrate phosphorylation, cellular glucose homeostasis, and trehalose biosynthetic process (Figure 5a). These observations led us to establish a positive expression association between *TaTPP-7A* in the Tre pathway and SnRK family members involved in the carbohydrate energy metabolism pathway since several studies have reported that the sugar signal of T6P directly inhibited SnRK1 activity in vitro both in *Arabidopsis* (Zhang *et al.*, 2009) and wheat grains (Martínez-Barajas *et al.*, 2011). As shown in Figure 5b, the association coefficient between *TaTPP-7A* and *SnRK2-2B* expressions in the transgenic OE lines (R^2 = 0.8208) was much higher

© 2023 The Authors. *Plant Biotechnology Journal* published by Society for Experimental Biology and The Association of Applied Biologists and John Wiley & Sons Ltd., 1–17

14677652, 0, Downloaded from https://onlinelibrary.wiley.com/doi/10.1111/pbi.14025 by Chinese Academy Of, Wiley Online Library on [15/03/2023]. See the Terms and Conditions (https://onlinelibrary.wiley.com/terms-and-conditions) on Wiley Online Library for rules of use; OA articles are governed by the applicable Creative Commons License

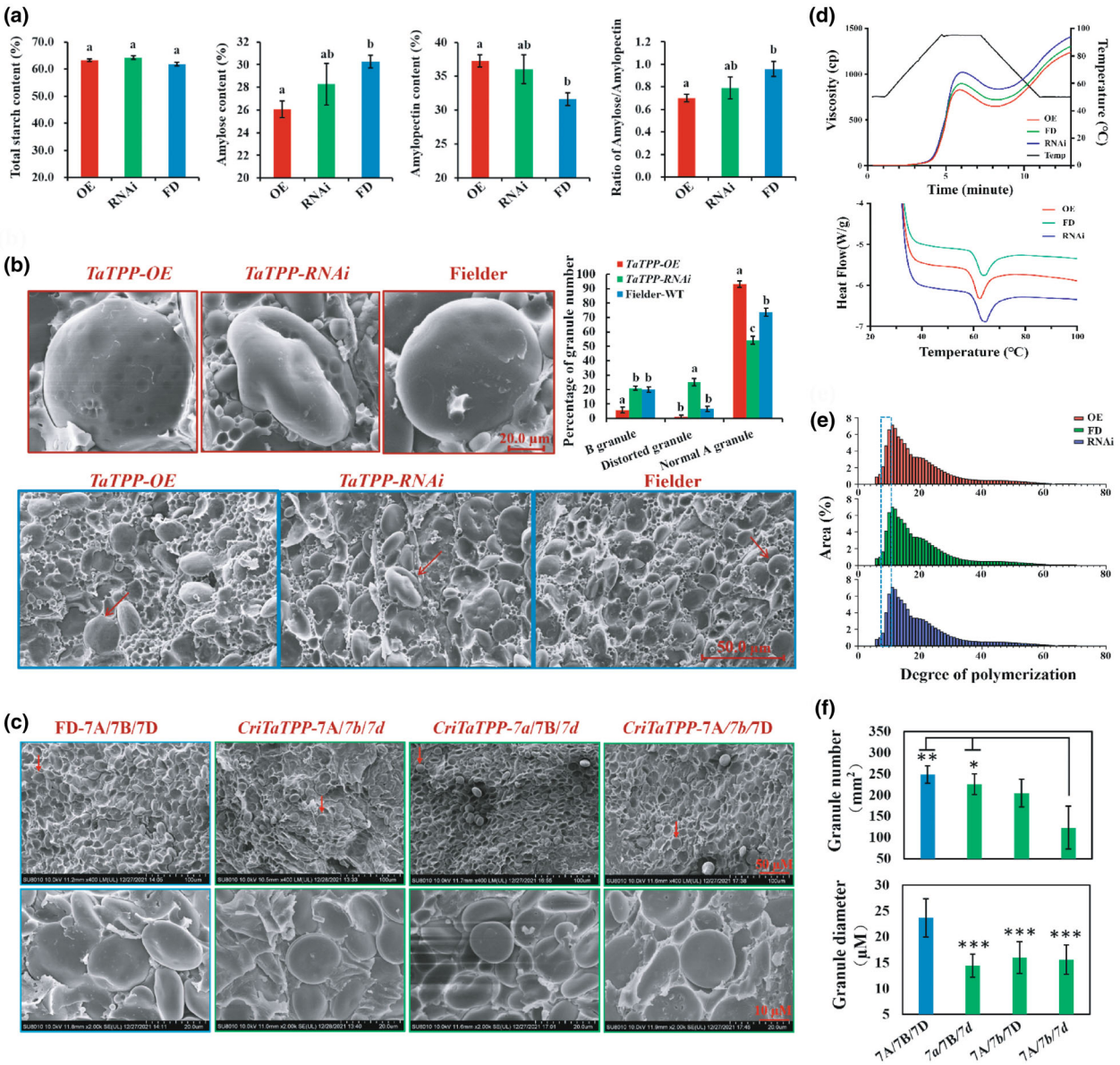

Figure 4 Starches physicochemical properties and granule characteristics (a) Total starch, amylose, and amylopectin content and the amylose/amylopectin ratio in the *TaTPP-7A* OE lines, RNAi lines, and the WT plants. Lowercase letters denote significant differences at $P < 0.05$. The difference is not significant with the same letter in pairwise comparison. (b, c) Scanning electron microscopy (SEM) images of starch granules from the mature grains of OE, RNAi, and *CriTaTPP* lines and WT plants. Red arrows indicate the selected enlarged granules. Scale bars, 10, 20, and 50 μM. Four grains were used for the analysis ($n = 4$). (d) Grain viscosity and gelatinization temperature. (e) Starch chain length distribution. The blue box indicates the most remarkable difference in starch chain length at DP 6–12 among the different transgenic lines. (f) Granule number and diameter in *CriTaTPP*s lines. *, **, and *** Denote statistically significant differences at $P < 0.05$, $P < 0.01$, and $P < 0.001$.

than that in WT plants ($R^2 = 0.6275$), indicating it was the OE of *TaTPP-7A* and the decrease in T6P that caused the increase in the association coefficient, and thus proved the possibility of T6P–SnRK1 interaction in vivo. Subsequently, based on the T6P–SnRK1 interaction model and the pioneering results on T6P accumulation in developing wheat grains by Martínez-Barajas *et al*. (2011), we found that about 7.69%–50% of the genes in different metabolic pathways may be regulated by SnRK1 (Figure 5c, Figure S14, SnRK1-dependent genes indicated by red dot); this set included genes related to sucrose lysis and transport and starch regulation (especially senescence- or abscisic acid (ABA) and ethylene pathway-associated genes). Detailed analysis revealed that the expression levels of the sucrose synthase (SUS) gene *SUS-2D*, sucrose transport (SUT) gene *SUT-2B*, ABA receptor gene *PYL3-7D*, and ethylene signal-responsive factor (ERF) gene *ERF-7D* enhanced about 9.4, 6.2, 13.1, and 272 times, respectively, at 5 DPA in the OE lines compared with the WT. One senescence-related gene *DUF581-6A/6B/6D*, with higher transcript levels in OE lines (75.57/70.10/59.55 times) than in WT at 5 DPA ($P < 0.05$ or $P < 0.01$; Figure 5c, starch regulation clade), also showed a clear SnRK1-dependent expression profile. These observations implied that *TaTPP-7A* might regulate grain

© 2023 The Authors. *Plant Biotechnology Journal* published by Society for Experimental Biology and The Association of Applied Biologists and John Wiley & Sons Ltd., 1–17

14677652, 0, Downloaded from https://onlinelibrary.wiley.com/doi/10.1111/pbi.14025 by Chinese Academy Of, Wiley Online Library on [15/03/2023]. See the Terms and Conditions (https://onlinelibrary.wiley.com/terms-and-conditions) on Wiley Online Library for rules of use; OA articles are governed by the applicable Creative Commons License

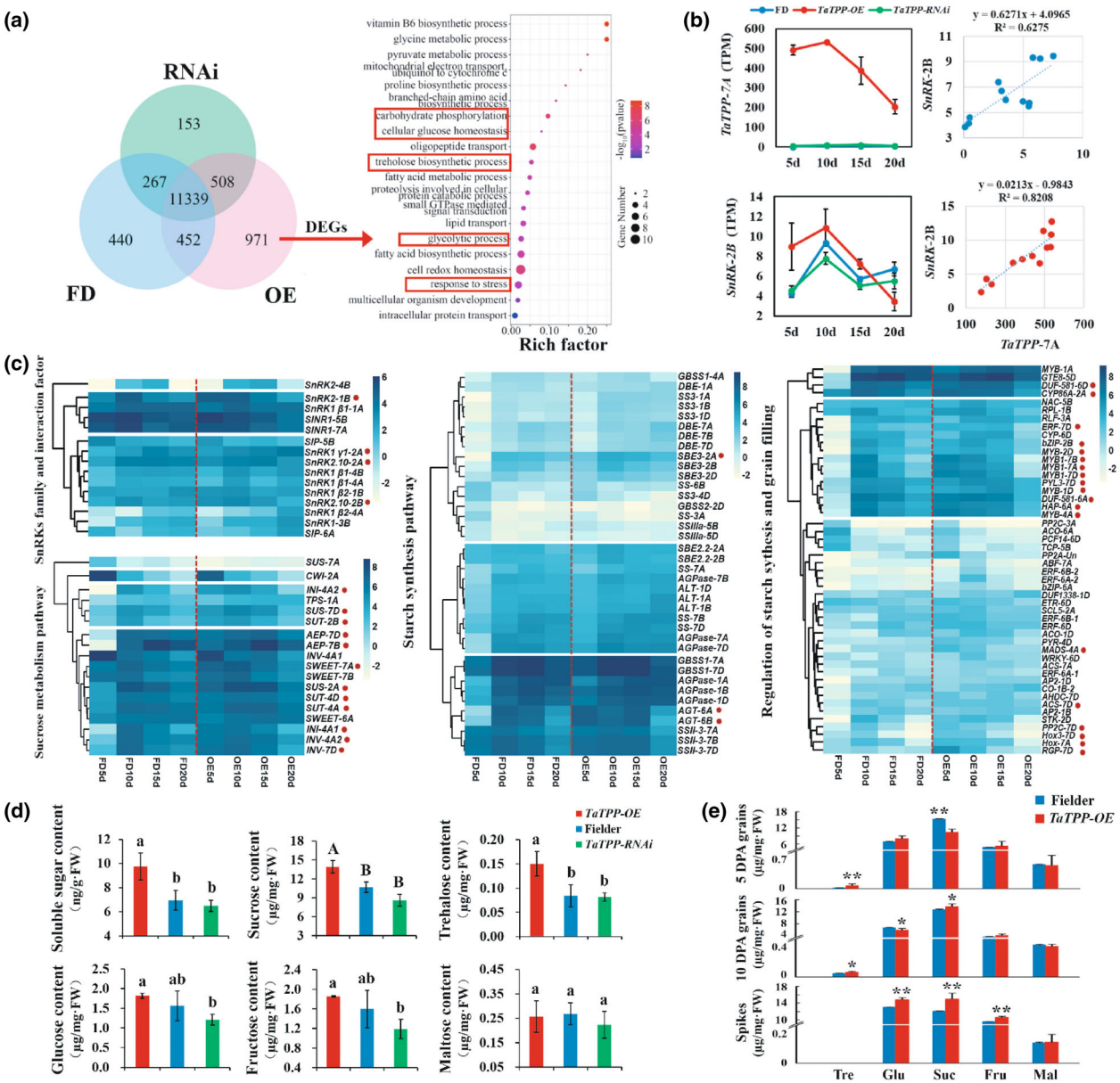

Figure 5 *TaTPP-7A*-mediated expression of downstream starch synthesis-related genes and sugar accumulation (a) Venn diagram and KEGG enrichment analysis of the DEGs among OE, RNAi lines, and WT plants. Red boxes indicate carbohydrate metabolism-related pathways. (b) Expression profile and association analysis between *SnRK2-2B* and *TaTPP-7A* in WT plants (blue dotted figure) and transgenic OE lines (red dotted figure). (c) Cluster heatmap analysis of the downstream genes regulated by *TaTPP-7A*. *SnRKs* family clade, sucrose metabolism clade, starch synthesis clade, and starch synthesis regulatory and grain filling clade are shown. Red dots denote the genes with SnRK1-dependent expression. The red dashed line demarcates FD (left) and the OE lines (right). (d, e) Content of total soluble sugars, sucrose, trehalose, and other sugars in fresh leaves, spikes, and grains. Bars indicate the standard error. Uppercase letters or ** and lowercase letters or * denote statistically significant differences at $P < 0.01$ and $P < 0.05$, respectively.

filling and maturity by affecting the levels of senescence hormones or/and senescence-related genes, consistent with the rapid grain filling phenotype of the OE lines (starting as early as 5 DPA). However, we also found about 58.4%–92.3% of DEGs were independent of this model. These DEGs included Myb transcription factor (TF) gene *Myb-1A*, Gibberellin 20 oxidase (GA20ox) gene *GA20ox-3B*, and Aldose 1-epimerase (AEP) gene *AEP-7B*, with 911.2, 377.9, and 823.9 times higher expression levels in the OE lines than those in WT at 5 DPA; their expression trends showed neither positive nor negative downstream genes associated with *SnRK1*. Surprisingly, we found that dozens of starch synthesis-related genes, such as ADP-glucose pyrophosphorylase (AGPase) gene *AGPase-1B/7D*, soluble starch synthase (SS) gene *SS3-1A*, granule-bound starch synthase (GBSS) gene *GBSS1-7A*, starch branching enzyme (SBE) gene *SBE3-2A*, and starch-debranching enzyme (DBE) gene *DBE-7D*, displayed significantly higher expression levels in transgenic OE lines than those in WT at 5 DPA; however, only *SBE3-2A* and ADPG transporter gene *TaBT1-6A/6B* showed SnRK1-dependent expression pattern, while the others did not, indicating T6P may directly regulate the expression of these genes or through some other unknown mechanism. Thus, our observations suggested that

© 2023 The Authors. *Plant Biotechnology Journal* published by Society for Experimental Biology and The Association of Applied Biologists and John Wiley & Sons Ltd., 1–17

14677652, 0, Downloaded from https://onlinelibrary.wiley.com/doi/10.1111/pbi.14025 by Chinese Academy Of, Wiley Online Library on [15/03/2023]. See the Terms and Conditions (https://onlinelibrary.wiley.com/terms-and-conditions) on Wiley Online Library for rules of use; OA articles are governed by the applicable Creative Commons License

both T6P and T6P–SnRK1 interactions are important components regulating wheat grain development.

We then evaluated the content of soluble carbohydrates in flag leaves, spikes, and grains to verify if *TaTPP-7A* affects sugar metabolism. We found significantly higher total soluble sugar, sucrose, and trehalose content in the leaves, spikes, and 10 DPA grains of the OE lines than in the WT ($P < 0.05$ and $P < 0.01$; Figure 5d,e), but significantly lower sucrose content in 5 DPA grains ($P < 0.01$). However, these observations are consistent with the expression of *SUS* genes and confirmed that *TaTPP-7A* affects sucrose lysis and utilization in wheat grains.

Domestication and breeding favour *TaTPP-7A* haplotypes related to TKW enhancement and early maturity

Genomic diversity and *haps* evolution of *TaTPP-7A* were evaluated using 262 MCC, 1347 modern cultivars, and a data set of 387 tetraploid/hexaploid accessions. Eight SNP variations, including three at the coding region and five at the promoter region, were found in the *TaTPP-7A* genomic sequence. These variations caused a mutation at 466 bp, changing Asp to Glu (aa 112), and 1278 bp, changing Ala to Val (aa 241), resulting in three *haps* among the 262 MCC (Figure 6a). Meanwhile, the five SNP variations in the promoter region affected the expression levels of *TaTPP-7A*, which was proven by the fluorescent signal in tobacco leaves carrying constructs with *Hap I* and *Hap II* promoters (Figure 6b).

The *Haps* association analysis showed that *TaTPP-7A* was significantly associated with high TKW and long GL ($P < 0.01$) both among the landraces and the modern cultivars under four environments (Table S4). Varieties with *Hap I* showed the highest TKW and the longest GL, whereas those with *Hap II* showed the lowest TKW and shortest grains. Meanwhile, varieties with *Hap III* displayed a moderate phenotype. The average difference in TKW and GL between *Hap I* and *Hap II* was about 8.25 g (7.63–8.94 g) and 6.6 mm (6.2–7.5 mm), respectively, within the landraces and 5.70 g (4.06–6.32 g) and 4.2 mm (3.5–4.8 mm), respectively, within the modern cultivars. In China, the frequency of *Hap I* has increased dramatically since the 1940s from 10.5% (0%–21.4%) in landraces to 65.4% (20%–100%) in modern cultivars across the ten wheat zones (Figure 6c,d, Figures S15, S16), whereas that of *Hap II* and *Hap III* decreased obviously from 58.3% (7.1%–100%) and 31.3% (0%–71%), respectively, in landraces, to 22.5% (0%–80%) and 12.0% (0%–50%), in modern cultivars. These observations indicated that *TaTPP-7A* had undergone an intense artificial selection during breeding in China. However, for the 384 foreign cultivars, especially for the germplasms in Mexico, Australia, Europe, and North America, the proportions of *Hap III* were higher than *Hap I* and *Hap II* (Figure 6f), indicating the differences in the haplotypes favoured in China and foreign countries.

Furthermore, results showed that the π value of *TaTPP-7A* decreased dramatically from landraces (0.0018) to modern cultivars (0.00139) ($P < 0.01$; Figure 1e). In addition, two dramatic declines in *TaTPP-7A Haps* diversity (H value) occurred during the *Triticum* genus evolution (Figure 6e, Figure S17), one at the tetraploid domestication stage ($P < 0.001$) and the other at the hexaploid breeding stage ($P < 0.01$); meanwhile, the *gHaps* (*haps* in hexaploid wheat) were derived clearly from the *aHaps* (*haps* in Emmer). These observations proved that *TaTPP-7A* is a crucial targeted gene continuously selected in wheat domestication and breeding.

Discussion

In wheat, grain TKW is a crucial factor influencing yield. Sucrose plays a vital role in determining TKW, however, the specific molecular mechanism regulating sucrose unloading and metabolism in grains remains largely unknown. In this study, we report firstly that the wheat gene *TaTPP-7A* feedback regulates sucrose lysis, flux, and utilization in grain endosperm through T6P-SnRK1 pathway and sugar–ABA interaction (Figure 7), and thus significantly enhanced grain filling and wheat yield under field condition. In *Arabidopsis* and rice, dozens of TKW-associated genes have been cloned and the possible mechanisms regulating grain size or filling were further analysed (Ashikari *et al*., 1999; Song *et al*., 2007; Wang *et al*., 2008, 2012b; Weng *et al*., 2008), but none of these genes have been identified as components of the Tre pathway. In addition, Tre components (T6P, *TPS*, and *TPP*) have been associated with an increase in yield in wheat (Zhang *et al*., 2017) and maize (Nuccio *et al*., 2015); however, the molecular mechanisms underlying these functions remain unclear. In the present study, the OE of *TaTPP-7A* in wheat resulted in a maximal 11.5 g higher TKW, and grain yield was enhanced by 24% compared with the WT. Further study demonstrated that Tre metabolic pathway might be the central regulatory system for sucrose allocation and sugar–ABA interactions in wheat grains. Therefore, our work highlights the importance of the T6P signalling pathway and reveals the role of the Tre pathway components in yield improvement.

TaTPP-7A synchronously controls sucrose lysis and starch synthesis through degrading T6P level and further promote sucrose flux

In plants, T6P has been widely accepted as an indicator of sucrose status and carbon availability in various plant species, such as potato (*Solanum tuberosum*) (Debast *et al*., 2011), cucumber (*Cucumis sativus*) (Zhang *et al*., 2015b), maize (*Z. mays*) (Henry *et al*., 2014), and wheat (Martínez-Barajas *et al*., 2011). In this study, we expected limited T6P content in the grains of the OE lines throughout the developing stages since *TaTPP-7A* directly dephosphorylates T6P, leading to low sucrose and high Tre content due to sucrose breakdown for subsequent grain filling. However, a significantly higher accumulation of both Tre and sucrose was detected in the OE wheat tissues, except for the grains at 5 DPA. The Tre and sucrose content in the developing grains (10 DPA) and flag leaves of OE lines were respectively about 22.1% and 8.1% ($P < 0.05$), 45.8% ($P < 0.05$) and 22.9% ($P < 0.01$) higher than those in the WT. Moreover, the sucrose content in the flag leaves and 10 DPA grains of the transgenic OE lines were 288 times and 93 times higher than the Tre content. Therefore, here sucrose content was more likely linked to the overall sugar status and response to low T6P levels than Tre content both in the source (leaves) and the sink (developing grains). In addition, we found the highest difference in the expression of sucrose lysis-related genes *TaSUS-2A/2B/2D* and *TaSUS-7D* in the grains at 5 DPA compared to the WT plants, which explains the great decrease in sucrose content of the OE lines at 5 DPA. Moreover, this difference suggests that the reduced T6P and sucrose level or T6P/sucrose ratio at 5 DPA signals a low sugar level or energy status to the source, leading to a continuous sucrose flux from leaves to grains. This conclusion is proved by the fact that the high expression levels of sucrose transporters, such as *TaSUT1-4A/4B/4D*, *TaSUT2-2B*, and *SWEET-*

© 2023 The Authors. *Plant Biotechnology Journal* published by Society for Experimental Biology and The Association of Applied Biologists and John Wiley & Sons Ltd., 1–17

14677652, 0, Downloaded from https://onlinelibrary.wiley.com/doi/10.1111/pbi.14025 by Chinese Academy Of, Wiley Online Library on [15/03/2023]. See the Terms and Conditions (https://onlinelibrary.wiley.com/terms-and-conditions) on Wiley Online Library for rules of use; OA articles are governed by the applicable Creative Commons License

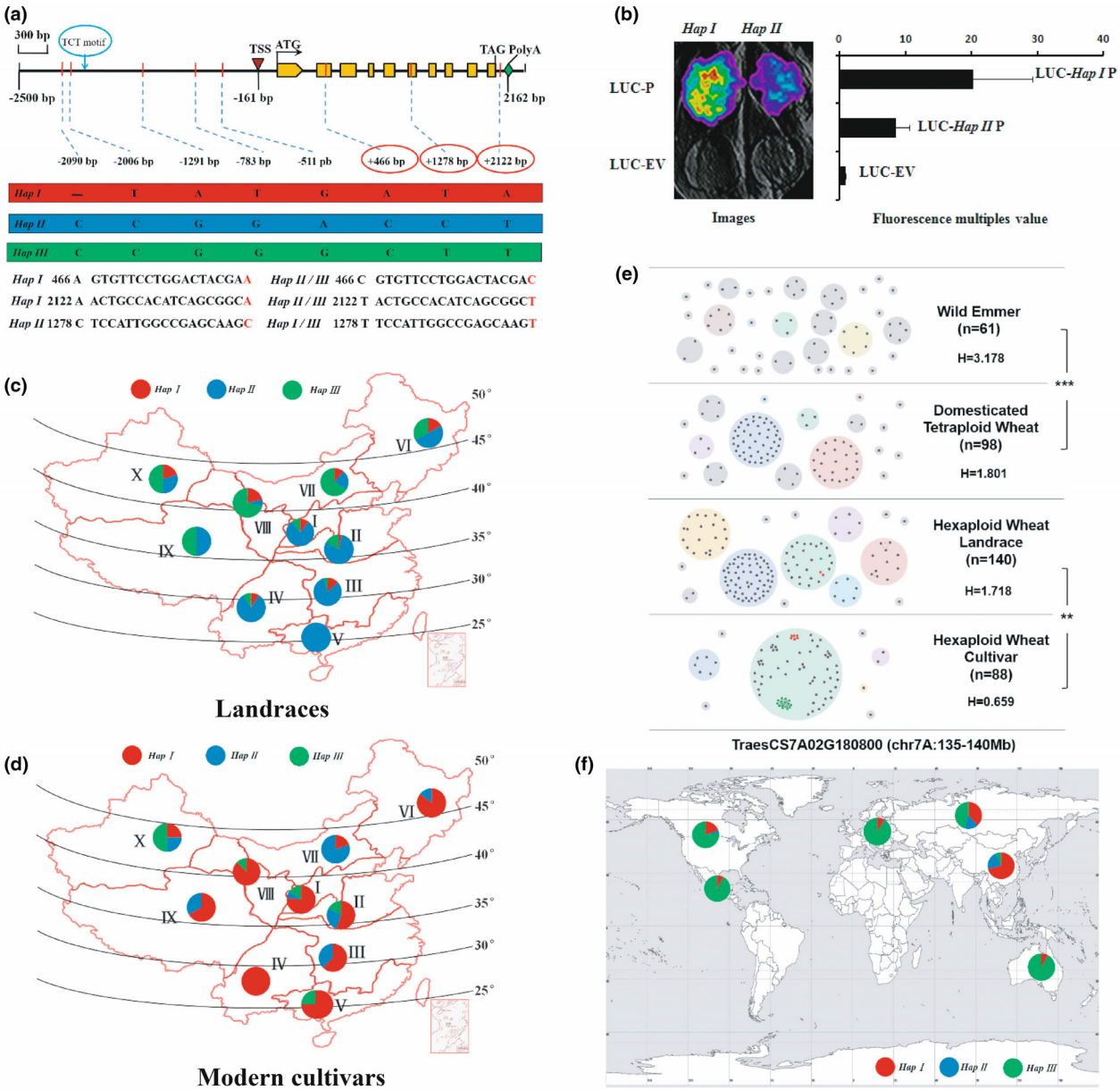

Figure 6 Haplotype diversity, domestication, and polyploidization analysis of *TaTPP-7A* (a) Schematic diagram shows the SNP variations and three haplotypes of *TaTPP-7A*. (b) Haplotype promoter activity. LUC-P/*-Hap I/II*-P denotes the fusion vector with the promoter of different haplotypes; LUC-EV denotes the empty vector. (c, d, f) Geographic distribution of *TaTPP*-7A haplotypes within Chinese landraces (157 accessions) and modern cultivars (105 accessions) and across other parts of the world (1347 wheat modern cultivars including 348 Chinese, 384 European, 429 North American, 53 CIMMYT, 82 Russian, and 51 Australian cultivars). (e) Domestication and polyploidization of *TaTPP-7A* haplotypes. Each dot denotes a single accession. Linked dots denote *gHaps* (hexaploid wheat), while circles denote *aHaps* (wild Emmer). Different colours denote different haplotypes. Haplotypes with the same colour in emmer, tetraploid, and hexaploid wheat populations are the same. H, Haplotype Shannon diversity index. Hutcheson's *t*-test was used to determine statistically significant differences; **, $P < 0.01$; ***, $P < 0.001$.

7A/*7B*/*6A*, were detected at 5 DPA in the OE lines. *TaSUT1* is a plasma membrane-localized transporter involved in the phloem loading of sucrose (Aoki *et al*., 2002), while *TaSUT2* controls the cytosolic sucrose homeostasis in flag leaves and grains (Deol *et al*., 2013). Therefore, the enhanced expression of *TaSUT1* and *TaSUT2* indicated the allocation of assimilates from the source to the sink (Aoki *et al*., 2002; Deol *et al*., 2013). In addition, this conclusion was also solidly supported by the effect of a rice *TPP1* on sucrose transport in maize, which highlighted seven *SWEETs* upregulated by *TPP1* in carbon partitioning for maize seed development (Oszvald *et al*., 2018). Thus, the increase in the sucrose content in wheat grains was more likely due to carbohydrate flux and not de novo synthesis.

In most plants, higher sucrose content is associated with the induction of starch synthesis. In this process, *SUS*, *AGPase*, or *TaBT1* plays essential roles (Kumar *et al*., 2018). Studies have shown that the OE of *SUS*, *AGPase*, or *TaBT1* in potato and wheat increased the starch content and TKW (Baroja-Fernández *et*

© 2023 The Authors. *Plant Biotechnology Journal* published by Society for Experimental Biology and The Association of Applied Biologists and John Wiley & Sons Ltd., 1–17

14677652, 0, Downloaded from https://onlinelibrary.wiley.com/doi/10.1111/pbi.14025 by Chinese Academy Of, Wiley Online Library on [15/03/2023]. See the Terms and Conditions (https://onlinelibrary.wiley.com/terms-and-conditions) on Wiley Online Library for rules of use; OA articles are governed by the applicable Creative Commons License

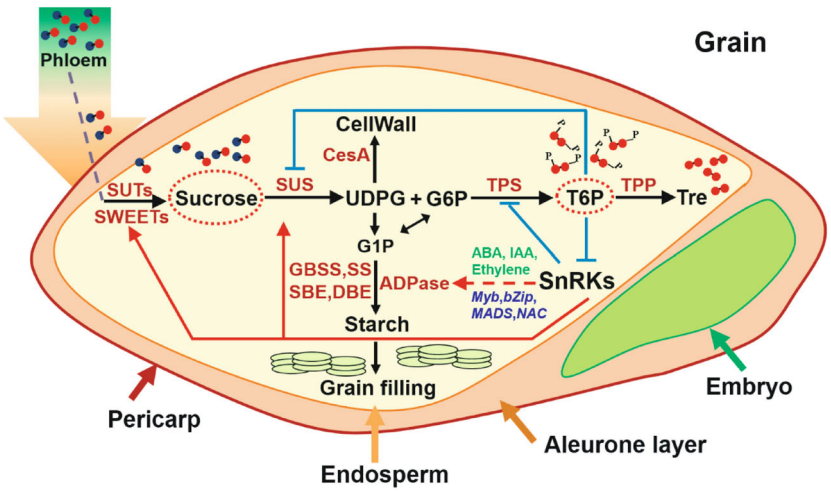

Figure 7 Model depicting the role of *TaTPP-7A* in enhancing wheat yield and grain filling In common wheat, during the early grain development stages (5–7 DPA), high levels of T6P inhibit SnRK1 activity in response to sucrose availability and promote carbon biosynthetic pathways (nucleotide and amino acid metabolism, cell wall and sucrose synthesis, and light reaction) (Zhang *et al*., 2009) for endosperm development. Subsequently (10 DPA), the dramatic drop in T6P levels activates SnRK1, triggering genes, hormones, and transcription factors dependent on SnRK1 and related to starch synthesis and systematically initiating grain filling and maturation. However, low T6P levels in the OE grains due to the dephosphorylation role of *TaTPP-7A* probably triggered three responses: (1) signal a low energy status in the sink to the source, leading to a continuous flux of sucrose from leaves to grains and (2) release of SnRK1 activity, enhancing sucrose transport (*SUT*, *SWEET*), lysis (*SUS*), and utilization (*TaBT1*, *SBE3*, *CesA*). (3) High sucrose and/or ABA and/or ethylene levels, inducing starch synthesis-related genes (*AGPase-L*, *AGPase-S*, *SS*, *GBSS*, *SBE*, *DBE*) or regulatory genes (*Myb*, *bZIP*, *MADS*, *NAC*) and promoting grain filling, maturation, and yield. Black arrows denote the metabolic steps. UDPG, G1P, and G6P are substrates and intermediate metabolites. Red arrows mark the activation effect. Blue and dashed lines represent the inhibitory effect.

al., 2009; Smidansky *et al*., 2002), which is consistent with our observations. The transgenic OE grains exhibited higher expression levels of *TaSUS-7D/2A*, *TaAGPase-S-7A/7B/7D*, *TaAGPase-L-1A/1B/1D*, *TaBT1*, and other starch synthesis-related genes, such as *SS*, *GBSS*, *SBE*, and *DBE*, especially at 5 DPA, indicating these genes as the targets of *TaTPP-7A*. Additionally, sucrose lysis at 5 DPA might have provided more UDPG substrate for starch synthesis than other DPA. Consistently, the total starch content of the OE lines was 2.53% higher than that of WT, indicating *TaTPP-7A* affects sucrose lysis and starch synthesis synchronously. In this study, we also detected a significant decrease in amylose content (13.2%) in the OE line compared with the WT. Moreover, the expression levels of *GBSS1-7A*, involved in amylose synthesis, were 3.14 times higher than the WT at 5 DPA, whereas that of *SBE3-2A*, responsible for amylopectin synthesis (Pérez *et al*., 2019), was 44.4 times higher and showed SnRK1-dependence. Thus, the higher expression difference in these genes might have resulted in starch granules with very low amylose but a higher amylopectin content in the grains of OE lines.

TaTPP-7A feedback affects sucrose lysis and starch synthesis mainly through the T6P-SnRK1 pathway and sugar–ABA interaction

Based on our findings and other reports, we confirmed the possibility of T6P–SnRK1 interaction in regulating wheat grain development in vivo. We found that most of the sucrose lysis and transport genes and several TFs showed a jumped and SnRK1-dependent expression pattern. In rice, maize, and wheat, SnRK1 directly activates the expression of genes encoding sucrose synthase (*SuSy*) (Smidansky *et al*., 2002, 2003) and sugar transporter (*SUT1*) (Bledsoe *et al*., 2017). Meanwhile, OE of SnRK1 stimulated starch synthesis in potato tubers and barley, leading to high starch accumulation through the redox activation of *AGPase* (McKibbin *et al*., 2006; Sreenivasulu *et al*., 2006). Thus, our observations might suggest that SnRK1 could also directly regulate sucrose metabolism-related genes in wheat, proving the role of T6P–SnRK1 interaction in grains. In addition, the high expression of the senescence-related protein gene, *DUF581-6A/6B/6D*, may also imply the role of T6P-SnRK1 pathways in regulating wheat grain filling. In *Arabidopsis*, this protein interacts with the catalytic α subunits of SnRK1 (AKIN10/11) (Nietzsche *et al*., 2016) and acts as a mediator or scaffold connecting the SnRK1 pathway with other signalling pathways, such as hormone, TOR, and MAP-kinase signalling pathways. Therefore, the DUF581 protein might have a function similar to that in *Arabidopsis* and confer stimulus-specific and tissue-specific differences in SnRK1 regulation in wheat.

In plants, the SnRK family comprises three subfamilies: SnRK1, SnRK2, and SnRK3. SnRK1 plays a major role in regulating carbon metabolism, while SnRK2 and SnRK3 have been implicated in ABA-mediated signalling pathways (Kong *et al*., 2015). Generally, SnRK2 activation is dependent on the breakdown of SnRK1 (Coello *et al*., 2012; Cutler *et al*., 2010). The present study found SnRK1-dependent expression for *PYL3-7D*, *PP2C-7D*, and *SnRK2-1B*, with 13, 11, and 3.2 times higher levels in OE lines than those in WT at 5 DPA. In addition, the expression levels of *NCED-5A/5B/5D*, the key speed-limiting enzyme of the ABA biosynthetic pathway, were also higher (5.0, 6.1, and 3.5 times) than those of WT at 5 DPA. These observations suggest that SnRK1 activated ABA signalling pathways during grain filling, and thus ABA plays important role in regulating grain filling. Therefore, TFs involved in the ABA pathway and regulated by SnRK1 might more likely contribute to the regulation of grain filling. The present study

© 2023 The Authors. *Plant Biotechnology Journal* published by Society for Experimental Biology and The Association of Applied Biologists and John Wiley & Sons Ltd.

14677652, 0, Downloaded from https://onlinelibrary.wiley.com/doi/10.1111/pbi.14025 by Chinese Academy Of, Wiley Online Library on [15/03/2023]. See the Terms and Conditions (https://onlinelibrary.wiley.com/terms-and-conditions) on Wiley Online Library for rules of use; OA articles are governed by the applicable Creative Commons License

found higher expression of *bZIP-2B* (basic leucine zipper) and *Myb-2D/4A/7A* at 5 DPA in the OE lines (218.0 and 361.6/132.2/120.4 times) than those in WT, clearly indicating SnRK1-dependent expression pattern. Studies have shown that SnRK1 mainly targets the members of the bZIP TF family in regulating plant growth and stress response under sugar starvation conditions (Hanson *et al*., 2008). Many ABA-regulated genes also contain binding sites for the MYB and MYC protein families (Cutler *et al*., 2010). Moreover, ABA has been demonstrated that involved in SnRK-related sugar signalling and promotes starch accumulation in developing seeds (Cutler *et al*., 2010). Thus, the enhanced TFs or genes controlled by SnRK1 in the OE lines may regulate grain filling too through the ABA pathway. In barley, ABA-responsive and dehydration-responsive *cis*-elements have been found in the promoters of key genes involved in starch biosynthesis (*HvSUS1* and *HvAGP-L1*) and degradation (*HvBAM1*) (Govind *et al*., 2011). In wheat and rice, ABA affects the transcriptional regulation of *SUS* (Yang *et al*., 2006; Zhu *et al*., 2011). In barley seeds, ABA homeostasis regulates starch accumulation rate and grain filling under drought (Govind *et al*., 2011) and modulates starch synthesis via SNF1 kinase and a few TFs (Sreenivasulu *et al*., 2006). These earlier reports support our results and confirm the role of SnRK1 or the ABA pathway in regulating starch synthesis. Thus, the present study proves that *TaTPP-7A* enhances wheat yield through senescence-related hormone biosynthesis and signalling and sugar–ABA interaction.

TaTPP-7A promotes grain filling and maturity probably via a synergistic effect on ABA and ethylene

ABA and ethylene are the major regulators of plant senescence (Cutler *et al*., 2010; Yang *et al*., 2006). Studies have shown that at the rapid grain-filling stages, ABA accumulation in the developing seeds regulates reserve remobilization and grain filling in barley, rice, and wheat (Govind *et al*., 2011; Yang *et al*., 2004, 2006). Meanwhile, the grain ethylene concentration has been negatively correlated with the grain-filling rate. In rice, ethylene concentrations are high at the early grain-filling stages and decrease sharply during the linear growth phase (Yang *et al*., 2004). However, in the present study, both ABA and ethylene appeared to play positive roles in regulating grain filling. The expression levels of ethylene biosynthesis-related genes *ACS-7D* (ACC synthase gene) and *ACO-1D* (ACC oxidase gene) and the ethylene-responsive factor *ERF-7D* enhanced synchronously with the ABA pathway-associated genes (more than five times) at 5 DPA and remained high till 15 DPA in the transgenic OE lines compared with those in WT. Especially for *ERF-7D*, the expression levels were 272 and 2.3 times higher at 5 and 15 DPA, indicating that the ethylene levels may not decrease during the early and late grain filling stages, which is in contrast to the findings of Yang *et al*. (2004) in rice. However, we found that the expression trends of ABA-related and ethylene-related genes in the OE grains were quite different; a gradual decrease was observed for the ABA signalling-related genes, such as *PYR-4D*, *PP2C-7D*, and *SnRK2-1B*, after anthesis, whereas a sharp decline was observed for the ethylene pathway-related genes, such as *ERF-7D* and *ACO*-1D, until 15 DPA, indicating that the concentrations and the balance between ethylene and ABA in the grains are necessary for grain filling. These findings suggest that accelerating the biosynthesis or signal transduction of senescence-related hormones at grain filling may be one of the ways via which *TaTPP-7A* synchronously enhanced grain filling and maturation.

Different *haps* of *TaTPP-7A* provide options to cope with the adverse effects of global warming via an 'escape' strategy

Grain filling is a key determinant of wheat productivity. A growing body of research has highlighted the link between genes regulating grain filling and domestication traits since the crops with larger seeds and higher yield have been selected as per human demands. In maize, the genes of the Tre pathway have been listed as candidates for domestication improvement; however, the link with the traits has not been reported (Hufford *et al*., 2012). The present study found that the wheat grain-filling gene, *TaTPP-7A*, has already been targeted during domestication and breeding in China, contributing to higher TKW and earlier maturity date (MD) traits. However, the importance of Tre pathway-related genes has just been recognized. We found that the H value of *TaTPP-7A haps* diversity in wild emmer wheat was significantly higher than that in the tetraploid and hexaploid wheat, which means *TaTPP-7A* was continuously under intense breeding selection, together with the downstream starch and sucrose metabolism-related genes (*TaAGPase-L* and *TaAGPase-S* (Hou *et al*., 2017), *TaSUS1* and *TaSUS2* (Hou *et al*., 2014)) and ADP-glucose transport gene *TaBT1* (Wang *et al*., 2019b), contributing to wheat yield improvement. Thus, the Tre pathway may be central in regulating sugar utilization and starch synthesis in wheat grains.

Furthermore, we found that the *Hap III* of *TaTPP-7A* in foreign wheat germplasm, especially the cultivars in Mexico, Europe, and North America, was favoured differently with China. Among the landraces of China, *Hap II* and *Hap III* of *TaTPP-7A* showed remarkable differences ($P < 0.01$) in heading date (HD) and MD under three environments. The HD and MD in varieties with *Hap III* were delayed by about 3.72 days (2.79–4.9 days) and 3.37 days (2.05–5.25 days), respectively, compared with the ones with *Hap II* (Table S4), thus, *Hap III* is beneficial for grain filling. However, the ongoing climate changes, such as high temperature and drought, occur more frequently and severely than before at wheat heading and filling stages (Marmai *et al*., 2022), and has posed a significant threat to wheat production. During 1964–2007, about 497 droughts and 138 extreme heat weather disasters occurred worldwide, leading to a 9%–10% decrease in cereal production (Lesk *et al*., 2016). A 4.1%–6.4% decrease in wheat production is estimated for every 1°C increase in global temperature due to climate change (Liu *et al*., 2016). Therefore, the development and utilization of early maturing varieties that 'escape' better than 'tolerate' heat stress and drought in hotter and drier summers are crucial for high crop yield; thus, the different *haps* of *TaTPP-7A* may be considered to improve wheat adaptation or output under climate changes. The present study found that the haplotype diversity of the *TaTPP-7A* gene between the domesticated tetraploid wheat and hexaploid landraces was almost the same, which indicates that this gene maintained abundant genetic diversity in landraces and thus could be further utilized for breeding other traits.

In conclusion, *TaTPP-7A* is a crucial domestication- and breeding-targeted gene in China and feedback regulates sucrose lysis, flux, and utilization in the grain endosperm mainly through T6P-SnRK1 pathway and sugar–ABA interaction. Thus, the present paper highlights the importance of the T6P signalling pathway and establishes Tre metabolic pathway as the central regulatory system for sucrose allocation and source–sink interactions in wheat grains. The study also proposes Tre pathway components as potential

© 2023 The Authors. *Plant Biotechnology Journal* published by Society for Experimental Biology and The Association of Applied Biologists and John Wiley & Sons Ltd.,

14677652, 0, Downloaded from https://onlinelibrary.wiley.com/doi/10.1111/pbi.14025 by Chinese Academy Of, Wiley Online Library on [15/03/2023]. See the Terms and Conditions (https://onlinelibrary.wiley.com/terms-and-conditions) on Wiley Online Library for rules of use; OA articles are governed by the applicable Creative Commons License

targets to increase grain size and yield in wheat. However, the direct regulatory effect of SnRK1 or *TaTPP-7A* on the sucrose metabolism gene should be further investigated.

Methods

Plant materials and growth condition

Chinese wheat 262 MCC (Hou *et al*., 2014; Su *et al*., 2011) was used for candidate gene association mapping, 1347 modern cultivars (348 Chinese, 384 European, 429 North American, 53 CIMMYT, 82 Russian, and 51 Australian) for genotyping and haplotype association analysis, and 716 F_2 lines of the biparental population for BSR-seq derived from 2840 F_2 individuals produced by crossing 'Zhongyou9507' cultivar with 'Hongjinmai' landraces (Table S5, Figure S18), were cultivated in the fields of Luoyang (112°45′E, 34°62′N; Henan, China) during 2001–2002, 2004–2005, and 2005–2006 and Shunyi (116°43′E, 40°09′N; Beijing, China) and Xinxiang (113°54′E, 35°18′N; Henan, China) during 2014–2015, 2015–2016, and 2016–2017, under local water (2–3 times for each crop season) and fertilizer management practices. The planting was carried out as described by Su *et al*. (2011) and Li *et al*. (2022). During the growing seasons, the average temperature was 10–22 °C in Shunyi and 12–24 °C in Luoyang and Xinxiang.

The *TaTPP-7A* OE or RNAi transgenic wheat lines were planted in the Shunyi fields at the year of 2016–2017, 2017–2018, and 2018–2019 following local water and fertilizer management practices as above. The seeds of the transgenic lines were sown in four 2 m long rows with a row spacing of 30 cm; 20 seeds were sown per row. The CRISPR/Cas9-mediated *TaTPP* edited wheat lines (*Cri-TaTPPs*), the *TaTPP* mutant in the tetraploid spring wheat cultivar Kronos background (*K-TaTPPs*), and tobacco (*Nicotiana benthamiana*) plants to analyse the gene function and promoter activity were cultivated in the greenhouse with a 16 h/8 h photoperiod; the temperature of the greenhouse was maintained at 22/20 °C ± 1 °C for wheat and 24 °C ± 1°C for tobacco. The *K-TaTPP* and *Cri-TaTPP* mutants were self-pollinated to M_3 or T_3–T_4 generations for phenotype evaluation; PCR and sequencing were used to detect the targeted genome variations in each generation, using the WT Kronos or Fielder (FD) as control.

Evaluation of the transgenic phenotype

Plants from the homozygous transgenic OE and RNAi lines (T_7–T_9; 5–7 independent transgenic lines, with 10–20 individuals per line; 94 OE and 123 RNAi individuals in total), *Cri-TaTPP* mutants (30 individuals), and FD (41 plants) were randomly selected to investigate the agronomic traits, including SN, PH, SL, SLN, GN, TKW, GL, and GW (Figure S8, Table S6). TKW was measured using a WSEEN Rice Test System (Wseen, Zhejiang, China). The images of the developing grains were captured using a stereomicroscope (SteREo Discovery V20, Zeiss, Germany). The size and shape of the starch granules were observed with a scanning electron microscope (SEM; SU8010, Hitachi, Japan), following the Wang *et al*. (2019b) protocol. Image J software (V1.48, National Institutes of Health) was used to measure cell size and number.

Transgene vector construction and wheat transformation

The full-length of *TaTPP-7A* cDNA (1086 bp) was amplified and sequentially cloned into the pWMB110 vector (*Bam*H I/*Eco*R I sites) to obtain the *TaTPP-7A* OE construct; A 309 bp fragment derived from the *TaTPP-7A* cDNA (7–315 nucleotides) was amplified and sequentially cloned into the pWMB006 vector respectively at *Bam*H I/*Kpn* I and *Sac* I/*Spe* I sites in opposite directions, with an intron between them to create a hairpin structure, and then inserted into the binary vector pWMB111 to obtain the *TaTPP-7A*-RNAi construct. The single guide RNA (sgRNA) sequences were designed to target a conserved region in the third exon of *TaTPPs*, and the fragments of the active TaU6-sgRNA were amplified and inserted into CRISPR/Cas9 vector pJIT163-2NLSCas9 to obtain the fused expression vector pGE-sgRNA, this construct was used to edit *TaTPP-7A*/*7B*/*7D* and generate the *CriTaTPPs* lines. All constructs (OE/RNAi/CRISPR/Cas9) were transformed into the immature embryos of the wheat cultivar FD using *Agrobacterium*-mediated transformation, following the protocols described by Wang *et al*. (2017) and Wang *et al*. (2014). All primers used in constructing the above vectors and selecting the lines are listed in Table S7.

RNA isolation, reverse transcription, and quantitative real-time PCR (qRT-PCR)

Total RNA was isolated from the wheat leaf, stem, root, and grain tissues using the TIANGEN RNA Extraction Kit (Tiangen, Beijing, China). Approximately 2 μg of total RNA was reverse transcribed into the cDNA using the SuperScript III RT system (Invitrogen, Madison, WI), according to the manufacturer's instructions. Then, qRT-PCR was performed as described by Wang *et al*. (2019b) on an Applied Biosystems 7500 Real-time PCR system (Thermo Fisher), using actin as the housekeeping gene. The primers used are listed in Table S8.

cDNA library construction, RNA-seq, and BSR-seq

Total RNA was extracted from the grains of the F_2 biparental progeny ten DPA as described above. For RNA-seq, three independent progeny with grain TKW ≥45 g (HG 1–3) or < 35 g (LG 1–3) were randomly selected and sequenced separately. Meanwhile, for BSR-seq, RNA samples were extracted from the pooled grains of 32 progeny with TKW ≥58 g or <28 g at equimolar amounts to obtain the highest bulks (CH) and the lowest bulks (CL), respectively. Six (HG 1–3 and LG 1–3, RNA-seq) and four (two bulks and two parents, BSR-seq) cDNA libraries were constructed using the TruSeq Stranded mRNA LT Sample Prep Kit (Illumina, San Diego, CA) according to the manufacturer's instructions, and sequenced separately on an Illumina platform (Illumina novaseq™ 6000) at the Beijing Biomics Technology Company Limited (Beijing, China) using the paired-end technology. The clean reads (Table S9) were assembled and aligned to the CS wheat reference genome sequence (RefSeq V1.0 and V2.1) released from the International Wheat Genome Sequencing Consortium (IWGSC) in 2018 (Appels *et al*., 2018).

The genes with a fold change (FC) ≥ 2 in RNA-seq data or ≥1.5 in BSR-seq data and a false discovery rate (FDR) < 0.01 were identified as the DEGs by DESeq2 (V1.10.1) (Anders and Huber, 2010). The differences in FPKM (the fragments per kilobase of transcript per million mapped reads) or TPM (transcripts per million reads) values were calculated using the EBseq software (V1.12.0) (Leng *et al*., 2013). DEGs were annotated based on the GO, COG (Clusters of Orthologous Groups of proteins), KOG (EuKaryotic Orthologous Groups), and KEGG (Kyoto Encyclopedia of Genes and Genomes) public databases. For BSR-seq analysis, the expression differences of the DEGs between the parents (PL_vs_PH_$\log_2$ (FC)) and the bulks (CL_vs_CH_$\log_2$ (FC)) were determined and compared, and those with a threshold $\log_2$ (FC) ≥ 0.5 and an expression difference

© 2023 The Authors. *Plant Biotechnology Journal* published by Society for Experimental Biology and The Association of Applied Biologists and John Wiley & Sons Ltd.

14677652, 0, Downloaded from https://onlinelibrary.wiley.com/doi/10.1111/pbi.14025 by Chinese Academy Of, Wiley Online Library on [15/03/2023]. See the Terms and Conditions (https://onlinelibrary.wiley.com/terms-and-conditions) on Wiley Online Library for rules of use; OA articles are governed by the applicable Creative Commons License

consistent for the parents and bulks were considered as the candidate genes.

Further, to analyse the downstream genes regulated by *TaTPP-7A*, total RNA was extracted from the transgenic and FD grains at 5, 10, 15, and 20 DPA and analysed via RNA-seq. The expression levels of DEGs (TPM) between the transgenic OE lines and the FD plants (Table S10) were presented as a cluster heat map using the Edge R software (V1.3.1093.0).

GWAS and genome diversity analysis

Chinese 262 MCC was chosen for GWAS of TKW using 984 034 SNPs captured by exome sequencing (Li *et al*., 2022). The association analysis was performed using the EMMAX software package (Kang *et al*., 2010). The pairwise LD coefficient (r^2) between SNPs was calculated using Plink (Purcell *et al*., 2007). Nucleotide diversity (π) was estimated using VCFtools (V 0.1.14) to assess the degree of variability within the landraces and the modern cultivars. The mean value and the best linear unbiased prediction (BLUP) value for the TKW trait at the same site and at different ages were calculated to perform GWAS.

Protein sequence alignment and phylogenetic analysis of *TPP* family

Protein sequences of *TPPs* in wheat, rice, *Arabidopsis*, and maize were retrieved from the Ensemble Plants public database (http://plants.ensembl.org/) and aligned using ClustalX, and the phylogenetic tree was constructed based on the neighbour-joining method with 1000 bootstrap replicates using MEGA 7.0 software (V 7.0.26). The TaTPP homoeologous protein sequences were aligned using DNAMAN software (Lynnon Biosoft, Quebec, Canada). The accession numbers of the genes used in the phylogenetic analysis are listed in Table S11.

Analysis of the *TaTPP* homoeologous haplotypes and promoter activity

Genomic variations in *TaTPPs* were detected by aligning the 2.3 kb long genomic sequence and 2.5 kb long promoter sequence amplified from 34 wheat varieties (22 modern cultivars and 12 landraces from 262 MCC; primers are listed in Table S12). The resulting fragments were cloned and sequenced on an ABI3730 XI DNA Analyser (Applied Biosystems), and the sequence variants (SNPs/Indel) were detected using DNASTAR (http://www.dnastar.com/). Three pairs of Kompetetive allele-specific PCR (KASP) markers (Table S13) were designed to genotype the *Haps* of *TaTPP-7A* in 262 MCC and 1347 modern cultivars of wheat. The *Haps* association analysis was conducted following the method described by Ma *et al*. (2016). *Haps* evolution was analysed using 387 tetraploid/hexaploid wheat accessions divided into four groups as follows: wild emmer ($n = 61$), domesticated tetraploid ($n = 98$), hexaploid landrace ($n = 140$), and hexaploid cultivar ($n = 88$). The ancestral-*haps* (*aHaps*) were inferred by IntroBlocker as described by Wang *et al*. (2022), while the germplasm-based *haps* (*gHaps*) for each 1 Mb bin were inferred using ggComp with default parameters as described by Yang *et al*. (2022). Finally, the Shannon diversity index of each group was calculated to determine the significance of the *haps* differences using the following formula:

$$H = -\sum_{i=1}^{L} p_i \ln(p_i),$$

where L refers to the count of *gHaps* for each bin, and p_i refers to the proportion of accessions in the i^{th} *gHap* in the whole panel.

The luciferase complementation imaging (LCI) assay was carried out to compare the promoter activities of the *TaTPP-7A haps*. Briefly, the *Hap 1* or *Hap 2* promoter sequence associated with the highest or lowest TKW was amplified by PCR as above and then introduced into the plant binary vector pGWB35-LUC to generate the fusion construct *TaTPP-Hap1pro*::LUC or *TaTPP-Hap2pro*::LUC, following the methods described by He *et al*. (2021). The *A. tumefaciens* (strain GV3101) cells carrying different constructs were infiltrated into *N. benthamiana* leaves, using cells with an empty vector (EV) as the negative control. The luciferase images were captured using a low-light-cooled CCD imaging apparatus (Night SHADE LB 985, Berthold, Bad Wildbad, Germany) and analysed with INDIGO software.

Determination of sugar and starch content and starches physicochemical properties

Soluble carbohydrates (sucrose, glucose, fructose, and trehalose) were extracted from 300 mg of the transgenic fresh leaves/grains/spikes following the method described by Lunn *et al*. (2006). The sugar content in the extract was determined by high-performance liquid chromatography (HPLC, Waters 600 controller) with an NH_2 column (5 mL, 4.6 mm × 250 mm I.D., Inertsil@ HPLC column) following the procedure described by Chang *et al*. (2013). Total starch and amylose in the endosperm were extracted and quantified following the Chinese national standard (NY/T11-1985, NY/T11-1987) for cereals with the optical rotation method. The thermal characteristics of the starch samples were analysed using a differential scanning calorimeter (DSC Q2000; TA Instruments, DE) according to the methods described by Lai *et al*. (2016). The gelatinization temperature and enthalpy were calculated using the Universal Analysis 2000 software (TA Instruments), and the pasting properties of the starch suspensions were determined using a Rapid Visco Analyser (RVA, MCR302, Anton Paar, Austria).

Statistical analysis

One-way analysis of variance (ANOVA) and Tukey's multiple comparison test were performed to determine data variance and significance ($*P < 0.05$, $**P < 0.01$, and $***P < 0.001$) using the SPSS 16.0 (SPSS). The Hutcheson *t*-test (Hutcheson, 1970) was applied to analyse statistical differences in the Shannon diversity index values between groups, using the *P*-value of a two-tailed test. All experiments were performed using no less than three replicates per sample, and the data were presented as the mean values ± standard deviation.

Acknowledgements

This study was supported by the National Natural Science Foundation of China (91935304 to HXL and 31471492 to HXL), the National Key Research and Development Program of China (2016YFD0100402 to HXL and 2016YFD0100302 to XYZ), the International Cooperation Program of the Ministry of Agriculture (2016-X16 to XYZ), and the CAAS-Innovation Program (HXL). We appreciate Dr. X.G. Ye (Institute of Crop Science, CAAS, China) for his help in wheat transformation. We are grateful to Researcher Z. F. Lu (Institute of Crop Sciences, CAAS, China) for the critical review of this manuscript.

Conflicts of interest

The authors declare no competing interests of this work.

© 2023 The Authors. *Plant Biotechnology Journal* published by Society for Experimental Biology and The Association of Applied Biologists and John Wiley & Sons Ltd.

14677652, 0, Downloaded from https://onlinelibrary.wiley.com/doi/10.1111/pbi.14025 by Chinese Academy Of, Wiley Online Library on [15/03/2023]. See the Terms and Conditions (https://onlinelibrary.wiley.com/terms-and-conditions) on Wiley Online Library for rules of use; OA articles are governed by the applicable Creative Commons License

Author contributions

H.X.L. conceived of the project, performed most experiments, and wrote the manuscript; X.M.S. constructed the F_2 segregation population and performed phenotype evaluation and genotype verification experiment; Z.Y.W. performed GWAS and fine-mapped the QTL; L.Y.C. performed grain quality experiment and transcriptome analysis; X.L.Z. and C.Z.J. assisted in BSR sequencing and data analysis; W.X.W. and W.L.G. conducted the analysis of haplotype domestication and polyploidization; L.F.G. and L.Z. assisted in genotyping and RNA-Seq. H.X.L. and K.W. developed the transgenic and CRISPR/Cas9 edited lines and performed the wheat transformation; Y.C.L. and J.H. performed qRT-PCR and phenotyping evaluation of transgenic lines in the laboratory and fields; C.Y.H., T.L., J.L., and W.L.G. provided advice about the experiments; X.Y.Z. revised the manuscript; all authors have read and approved the manuscript.

Data availability statement

The exome sequencing data, BSR-seq and RNA-seq data have been submitted to NCBI under the project numbers PRJNA550304, PRJNA879906, and PRJNA882584. Additional supporting information may be found online in the Supporting information section at the end of this article.

References

Anders, S. and Huber, W. (2010) Differential expression analysis for sequence count data. *Genome Biol.* **11**, R106.

Aoki, N., Whitfeld, P., Hoeren, F., Scofield, G., Newell, K., Patrick, J., Offler, C. *et al*. (2002) Three sucrose transporter genes are expressed in the developing grain of hexaploid wheat. *Plant Mol. Biol.* **50**, 453–462.

Appels, R., Eversole, K., Feuillet, C., Keller, B., Rogers, J., Stein, N., Pozniak, C. *et al*. (2018) Shifting the limits in wheat research and breeding using a fully annotated reference genome. *Science* **361**, aar7191.

Ashikari, M., Wu, J., Yano, M., Sasaki, T. and Yoshimura, A. (1999) Rice gibberellin-insensitive dwarf mutant gene *Dwarf 1* encodes the alpha-subunit of GTP-binding protein. *Proc. Natl. Acad. Sci. U. S. A.* **96**, 10284–10289.

Baroja-Fernández, E., Muñoz, F., Montero, M., Etxeberria, E., Sesma, M., Ovecka, M., Bahaji, A. *et al*. (2009) Enhancing sucrose synthase activity in transgenic potato (*Solanum tuberosum* L.) tubers results in increased levels of starch, ADPglucose and UDPglucose and total yield. *Plant Cell Physiol.* **50**, 1651–1662.

Bledsoe, S., Henry, C., Griffiths, C., Paul, M., Feil, R., Lunn, J., Stitt, M. *et al*. (2017) The role of Tre6P and SnRK1 in maize early kernel development and events leading to stress-induced kernel abortion. *BMC Plant Biol.* **17**, 74.

Chang, Q., Liu, J., Wang, Q., Han, L., Liu, J., Li, M., Huang, L. *et al*. (2013) The effect of *Puccinia striiformis* f. sp. tritici on the levels of water-soluble carbohydrates and the photosynthetic rate in wheat leaves. *Physiol Mol Plant Pathol.* **84**, 131–137.

Coello, P., Hirano, E., Hey, S., Muttucumaru, N., Martinez-Barajas, E., Parry, M. and Halford, N. (2012) Evidence that abscisic acid promotes degradation of SNF1-related protein kinase (SnRK) 1 in wheat and activation of a putative calcium-dependent SnRK2. *J. Exp. Bot.* **63**, 913–924.

Cutler, S., Rodriguez, P., Finkelstein, R. and Abrams, S. (2010) Abscisic acid: emergence of a core signaling network. *Annu. Rev. Plant Biol.* **61**, 651–679.

Debast, S., Nunes-Nesi, A., Hajirezaei, M., Hofmann, J., Sonnewald, U., Fernie, A. and Börnke, F. (2011) Altering trehalose-6-phosphate content in transgenic potato tubers affects tuber growth and alters responsiveness to hormones during sprouting. *Plant Physiol.* **156**, 1754–1771.

Deol, K., Mukherjee, S., Gao, F., Brûlé-Babel, A., Stasolla, C. and Ayele, B. (2013) Identification and characterization of the three homeologues of a new sucrose transporter in hexaploid wheat (*Triticum aestivum* L.). *BMC Plant Biol.* **13**, 181.

Fan, C., Xing, Y., Mao, H., Lu, T., Han, B., Xu, C., Li, X. *et al*. (2006) *GS3*, a major QTL for grain length and weight and minor QTL for grain width and thickness in rice, encodes a putative transmembrane protein. *Theor. Appl. Genet.* **112**, 1164–1171.

Figueroa, C. and Lunn, J. (2016) A Tale of Two Sugars: Trehalose 6-Phosphate and Sucrose. *Plant Physiol.* **172**, 7–27.

Godfray, H., Beddington, J., Crute, I., Haddad, L., Lawrence, D., Muir, J., Pretty, J. *et al*. (2010) Food security: the challenge of feeding 9 billion people. *Science* **327**, 812–818.

Govind, G., Seiler, C., Wobus, U. and Sreenivasulu, N. (2011) Importance of ABA homeostasis under terminal drought stress in regulating grain filling events. *Plant Signal. Behav.* **6**, 1228–1231.

Hanson, J., Hanssen, M., Wiese, A., Hendriks, M. and Smeekens, S. (2008) The sucrose regulated transcription factor *bZIP11* affects amino acid metabolism by regulating the expression of *ASPARAGINE SYNTHETASE1* and *PROLINE DEHYDROGENASE2*. *Plant J.* **53**, 935–949.

He, G., Zhang, Y., Liu, P., Jing, Y., Zhang, L., Zhu, Y., Kong, X. *et al*. (2021) The transcription factor *TaLAX1* interacts with *Q* to antagonistically regulate grain threshability and spike morphogenesis in bread wheat. *New Phytol.* **230**, 988–1002.

Henry, C., Bledsoe, S., Siekman, A., Kollman, A., Waters, B., Feil, R., Stitt, M. *et al*. (2014) The trehalose pathway in maize: conservation and gene regulation in response to the diurnal cycle and extended darkness. *J. Exp. Bot.* **65**, 5959–5973.

Hou, J., Jiang, Q., Hao, C., Wang, Y., Zhang, H. and Zhang, X. (2014) Global selection on sucrose synthase haplotypes during a century of wheat breeding. *Plant Physiol.* **164**, 1918–1929.

Hou, J., Li, T., Wang, Y., Hao, C., Liu, H. and Zhang, X. (2017) ADP-glucose pyrophosphorylase genes, associated with kernel weight, underwent selection during wheat domestication and breeding. *Plant Biotechnol. J.* **15**, 1533–1543.

Hu, M., Zhang, H., Liu, K., Cao, J., Wang, S., Jiang, H., Wu, Z. *et al*. (2016) Cloning and characterization of *TaTGW-7A* gene associated with grain weight in wheat via SLAF-seq-BSA. *Front. Plant Sci.* **7**, 1902.

Hufford, M., Xu, X., van Heerwaarden, J., Pyhäjärvi, T., Chia, J., Cartwright, R., Elshire, R. *et al*. (2012) Comparative population genomics of maize domestication and improvement. *Nat. Genet.* **44**, 808–811.

Hutcheson, K. (1970) A test for comparing diversities based on the Shannon formula. *J. Theor. Biol.* **29**, 151–154.

Jia, M., Li, Y., Wang, Z., Tao, S., Sun, G., Kong, X., Wang, K. *et al*. (2021) *TaIAA21* represses *TaARF25*-mediated expression of *TaERFs* required for grain size and weight development in wheat. *Plant J.* **108**, 1754–1767.

Kang, H., Sul, J., Service, S., Zaitlen, N., Kong, S., Freimer, N., Sabatti, C. *et al*. (2010) Variance component model to account for sample structure in genome-wide association studies. *Nat. Genet.* **42**, 348–354.

Kong, L., Guo, H. and Sun, M. (2015) Signal transduction during wheat grain development. *Planta* **241**, 789–801.

Kumar, R., Mukherjee, S. and Ayele, B. (2018) Molecular aspects of sucrose transport and its metabolism to starch during seed development in wheat: A comprehensive review. *Biotechnol. Adv.* **36**, 954–967.

Lai, Y., Wang, S., Gao, H., Nguyen, K., Nguyen, C., Shih, M. and Lin, K. (2016) Physicochemical properties of starches and expression and activity of starch biosynthesis-related genes in sweet potatoes. *Food Chem.* **199**, 556–564.

Leng, N., Dawson, J., Thomson, J., Ruotti, V., Rissman, A., Smits, B., Haag, J. *et al*. (2013) EBSeq: an empirical Bayes hierarchical model for inference in RNA-seq experiments. *Bioinformatics* **29**, 1035–1043.

Lesk, C., Rowhani, P. and Ramankutty, N. (2016) Influence of extreme weather disasters on global crop production. *Nature* **529**, 84–87.

Li, Y., Fan, C., Xing, Y., Jiang, Y., Luo, L., Sun, L., Shao, D. *et al*. (2011) Natural variation in *GS5* plays an important role in regulating grain size and yield in rice. *Nat. Genet.* **43**, 1266–1269.

Li, A., Hao, C., Wang, Z., Geng, S., Jia, M., Wang, F., Han, X. *et al*. (2022) Wheat breeding history reveals synergistic selection of pleiotropic genomic sites for plant architecture and grain yield. *Mol. Plant* **15**, 504–519.

Liu, B., Asseng, S., Muller, C., Ewert, F., Elliott, J., Lobell, D., Martre, P. *et al*. (2016) Similar estimates of temperature impacts on global wheat yield by three independent methods. *Nat Clim Change.* **6**, 1130–1136.

© 2023 The Authors. *Plant Biotechnology Journal* published by Society for Experimental Biology and The Association of Applied Biologists and John Wiley & Sons Ltd.

14677652, 0, Downloaded from https://onlinelibrary.wiley.com/doi/10.1111/pbi.14025 by Chinese Academy Of, Wiley Online Library on [15/03/2023]. See the Terms and Conditions (https://onlinelibrary.wiley.com/terms-and-conditions) on Wiley Online Library for rules of use; OA articles are governed by the applicable Creative Commons License

Liu, H., Li, H., Hao, C., Wang, K., Wang, Y., Qin, L., An, D. *et al*. (2020) *TaDA1*, a conserved negative regulator of kernel size, has an additive effect with *TaGW2* in common wheat (*Triticum aestivum* L.). *Plant Biotechnol. J.* **18**, 1330–1342.

Lunn, J., Feil, R., Hendriks, J., Gibon, Y., Morcuende, R., Osuna, D., Scheible, W. *et al*. (2006) Sugar-induced increases in trehalose 6-phosphate are correlated with redox activation of ADPglucose pyrophosphorylase and higher rates of starch synthesis in *Arabidopsis thaliana*. *Biochem. J.* **397**, 139–148.

Ma, L., Li, T., Hao, C., Wang, Y., Chen, X. and Zhang, X. (2016) *TaGS5-3A*, a grain size gene selected during wheat improvement for larger kernel and yield. *Plant Biotechnol. J.* **14**, 1269–1280.

Marmai, N., Franco-Villoria, M. and Guerzoni, M. (2022) How the Black Swan damages the harvest: Extreme weather events and the fragility of agriculture in development countries. *PLoS One.* **17**, e0261839.

Martínez-Barajas, E., Delatte, T., Schluepmann, H., de Jong, G., Somsen, G., Nunes, C., Primavesi, L. *et al*. (2011) Wheat grain development is characterized by remarkable trehalose 6-phosphate accumulation pregrain filling: tissue distribution and relationship to SNF1-related protein kinase1 activity. *Plant Physiol.* **156**, 373–381.

McKibbin, R., Muttucumaru, N., Paul, M., Powers, S., Burrell, M., Coates, S., Purcell, P. *et al*. (2006) Production of high-starch, low-glucose potatoes through over-expression of the metabolic regulator SnRK1. *Plant Biotechnol. J.* **4**, 409–418.

Nietzsche, M., Landgraf, R., Tohge, T. and Bornke, F. (2016) A protein-protein interaction network linking the energy-sensor kinase SnRk1 to multiple signaling pathways in *Arabidopsis thaliana*. *Current Plant Biol.* **5**, 36–44.

Nuccio, M., Wu, J., Mowers, R., Zhou, H., Meghji, M., Primavesi, L., Paul, M. *et al*. (2015) Expression of trehalose-6-phosphate phosphatase in maize ears improves yield in well-watered and drought conditions. *Nat. Biotechnol.* **33**, 862–869.

O'Hara, L., Paul, M. and Wingler, A. (2013) How do sugars regulate plant growth and development? New insight into the role of trehalose-6-phosphate. *Mol. Plant* **6**, 261–274.

Oszvald, M., Primavesi, L., Griffiths, C., Cohn, J., Basu, S., Nuccio, M. and Paul, M. (2018) Trehalose 6-phosphate regulates photosynthesis and assimilate partitioning in reproductive tissue. *Plant Physiol.* **176**, 2623–2638.

Paul, M. (2008) Trehalose 6-phosphate: a signal of sucrose status. *Biochem. J.* **412**, e1–e2.

Paul, M., Watson, A. and Griffiths, C. (2020) Trehalose 6-phosphate signalling and impact on crop yield. *Biochem. Soc. Trans.* **48**, 2127–2137.

Pérez, L., Soto, E., Farré, G., Juanos, J., Villorbina, G., Bassie, L., Medina, V. *et al*. (2019) CRISPR/Cas9 mutations in the rice *Waxy/GBSSI* gene induce allele-specific and zygosity-dependent feedback effects on endosperm starch biosynthesis. *Plant Cell Rep.* **38**, 417–433.

Pfeifer, M., Kugler, K., Sandve, S., Zhan, B., Rudi, H., Hvidsten, T., Mayer, K. *et al*. (2014) Genome interplay in the grain transcriptome of hexaploid bread wheat. *Science* **345**, 1250091.

Purcell, S., Neale, B., Todd-Brown, K., Thomas, L., Ferreira, M., Bender, D., Maller, J. *et al*. (2007) PLINK: a tool set for whole-genome association and population-based linkage analyses. *Am. J. Hum. Genet.* **81**, 559–575.

Sakamoto, T. and Matsuoka, M. (2008) Identifying and exploiting grain yield genes in rice. *Curr. Opin. Plant Biol.* **11**, 209–214.

Satoh-Nagasawa, N., Nagasawa, N., Malcomber, S., Sakai, H. and Jackson, D. (2006) A trehalose metabolic enzyme controls inflorescence architecture in maize. *Nature* **441**, 227–230.

Schluepmann, H. and Paul, M. (2009) Trehalose Metabolites in Arabidopsis-elusive, active and central. In *The Arabidopsis Book* (Last, R., Chang, C., Jander, G., Kliebenstein, D., McClung, R., Millar, H., Torii, K. *et al*., eds), pp. 1–17. Washington, DC: American Society of Plant Biologists.

Schluepmann, H., Pellny, T., van Dijken, A., Smeekens, S. and Paul, M. (2003) Trehalose 6-phosphate is indispensable for carbohydrate utilization and growth in *Arabidopsis thaliana*. *Proc. Natl. Acad. Sci. U. S. A.* **100**, 6849–6854.

Smidansky, E., Clancy, M., Meyer, F., Lanning, S., Blake, N., Talbert, L. and Giroux, M. (2002) Enhanced ADP-glucose pyrophosphorylase activity in wheat endosperm increases seed yield. *Proc. Natl. Acad. Sci. U. S. A.* **99**, 1724–1729.

Smidansky, E., Martin, J., Hannah, L., Fischer, A. and Giroux, M. (2003) Seed yield and plant biomass increases in rice are conferred by deregulation of endosperm ADP-glucose pyrophosphorylase. *Planta* **216**, 656–664.

Song, X., Huang, W., Shi, M., Zhu, M. and Lin, H. (2007) A QTL for rice grain width and weight encodes a previously unknown RING-type E3 ubiquitin ligase. *Nat. Genet.* **39**, 623–630.

Sreenivasulu, N., Radchuk, V., Strickert, M., Miersch, O., Weschke, W. and Wobus, U. (2006) Gene expression patterns reveal tissue-specific signaling networks controlling programmed cell death and ABA- regulated maturation in developing barley seeds. *Plant J.* **47**, 310–327.

Su, Z., Hao, C., Wang, L., Dong, Y. and Zhang, X. (2011) Identification and development of a functional marker of *TaGW2* associated with grain weight in bread wheat (*Triticum aestivum* L.). *Theor. Appl. Genet.* **122**, 211–223.

Wang, E., Wang, J., Zhu, X., Hao, W., Wang, L., Li, Q., Zhang, L. *et al*. (2008) Control of rice grain-filling and yield by a gene with a potential signature of domestication. *Nat. Genet.* **40**, 1370–1374.

Wang, L., Ge, H., Hao, C., Dong, Y. and Zhang, X. (2012a) Identifying loci influencing 1,000-kernel weight in wheat by microsatellite screening for evidence of selection during breeding. *PLoS One.* **7**, e29432.

Wang, S., Wu, K., Yuan, Q., Liu, X., Liu, Z., Lin, X., Zeng, R. *et al*. (2012b) Control of grain size, shape and quality by *OsSPL16* in rice. *Nat. Genet.* **44**, 950–954.

Wang, Y., Cheng, X., Shan, Q., Zhang, Y., Liu, J., Gao, C. and Qiu, J. (2014) Simultaneous editing of three homoeoalleles in hexaploid bread wheat confers heritable resistance to *powdery mildew*. *Nat. Biotechnol.* **32**, 947–951.

Wang, K., Liu, H., Du, L. and Ye, X. (2017) Generation of marker-free transgenic hexaploid wheat via an *Agrobacterium*-mediated co-transformation strategy in commercial Chinese wheat varieties. *Plant Biotechnol. J.* **15**, 614–623.

Wang, W., Pan, Q., Tian, B., He, F., Chen, Y., Bai, G., Akhunova, A. *et al*. (2019a) Gene editing of the wheat homologs of TONNEAU1-recruiting motif encoding gene affects grain shape and weight in wheat. *Plant J.* **100**, 251–264.

Wang, Y., Hou, J., Liu, H., Li, T., Wang, K., Hao, C., Liu, H. *et al*. (2019b) *TaBT1*, affecting starch synthesis and thousand kernel weight, underwent strong selection during wheat improvement. *J. Exp. Bot.* **70**, 1497–1511.

Wang, Z., Wang, W., Xie, X., Wang, Y., Yang, Z., Peng, H., Xin, M. *et al*. (2022) Dispersed emergence and protracted domestication of polyploid wheat uncovered by mosaic ancestral haploblock inference. *Nat. Commun.* **13**, 3891.

Weng, J., Gu, S., Wan, X., Gao, H., Guo, T., Su, N., Lei, C. *et al*. (2008) Isolation and initial characterization of *GW5*, a major QTL associated with rice grain width and weight. *Cell Res.* **18**, 1199–1209.

Xiao, S. and He, Z. (2003) Wheat yield and end use quality improvement in China. In *Chinese Wheat Improvement and Pedigree Analysis* (Zhuang, Q.S., ed), pp. 497–542. Beijing: China Agriculture.

Yan, X., Zhao, L., Ren, Y., Dong, Z., Cui, D. and Chen, F. (2019) Genome-wide association study revealed that the *TaGW8* gene was associated with kernel size in Chinese bread wheat. *Sci. Rep.* **9**, 2702.

Yang, J., Zhang, J., Ye, Y., Wang, Z., Zhu, Q. and Liu, L. (2004) Involvement of abscisic acid and ethylene in the responses of rice grains to water stress during filling. *Plant Cell Env.* **27**, 1055–1064.

Yang, J., Zhang, J., Liu, K., Wang, Z. and Liu, L. (2006) Abscisic acid and ethylene interact in wheat grains in response to soil drying during grain filling. *New Phytol.* **171**, 293–303.

Yang, Z., Wang, Z., Wang, W., Xie, X., Chai, L., Wang, X., Feng, X. *et al*. (2022) GGComp enables dissection of germplasm resources and construction of a multiscale germplasm network in wheat. *Plant Physiol.* **188**, 1950–1965.

Zhang, Y., Primavesi, L., Jhurreea, D., Andralojc, P., Mitchell, R., Powers, S., Schluepmann, H. *et al*. (2009) Inhibition of SNF1-related protein kinase1 activity and regulation of metabolic pathways by trehalose-6-phosphate. *Plant Physiol.* **149**, 1860–1871.

Zhang, L., Zhao, Y., Gao, L., Zhao, G., Zhou, R., Zhang, B. and Jia, J. (2012) *TaCKX6-D1*, the ortholog of rice *OsCKX2*, is associated with grain weight in hexaploid wheat. *New Phytol.* **195**, 574–584.

14677652, 0, Downloaded from https://onlinelibrary.wiley.com/doi/10.1111/pbi.14025 by Chinese Academy Of, Wiley Online Library on [15/03/2023]. See the Terms and Conditions (https://onlinelibrary.wiley.com/terms-and-conditions) on Wiley Online Library for rules of use; OA articles are governed by the applicable Creative Commons License

Zhang, D., Wang, B., Zhao, J., Zhao, X., Zhang, L., Liu, D., Dong, L. *et al.* (2015a) Divergence in homoeolog expression of the grain length-associated gene *GASR7* during wheat allohexaploidization. *Crop J.* **3**, 1–9.

Zhang, Z., Deng, Y., Song, X. and Miao, M. (2015b) Trehalose-6-phosphate and SNF1-related protein kinase 1 are involved in the first-fruit inhibition of cucumber. *J. Plant Physiol.* **177**, 110–120.

Zhang, P., He, Z., Tian, X., Gao, F., Xu, D. and Liu, J. (2017) Cloning of *TaTPP-6AL* associated with grain in bread wheat and developmentof functional marker. *Mol. Breeding.* **37**, 78.

Zhu, G., Ye, N., Yang, J., Peng, X. and Zhang, J. (2011) Regulation of expression of starch synthesis genes by ethylene and ABA in relation to the development of rice inferior and superior spikelets. *J. Exp. Bot.* **62**, 3907–3916.

Zuo, J. and Li, J. (2014) Molecular genetic dissection of quantitative trait loci regulating rice grain size. *Annu. Rev. Genet.* **48**, 99–118.

Supporting information

Additional supporting information may be found online in the Supporting Information section at the end of the article.

Figure S1 *TaTPP-7A* localization in wheat using nulli-tetrasomic lines of CS.

Figure S2 Collinearity analysis of *TaTPP-7A* (*Wmc17*) in wheat, rice, barley, *Arabidopsis thaliana*, and *Brachypodium*.

Figure S3 TKW differences between two parents and the derived F_2 segregation progeny for BSR-seq.

Figure S4 KEGG pathway enrichment analysis of the DEGs identified using BSR-seq data of the parental pool (PL vs. PH) and two bulks (CL vs. CH).

Figure S5 Expression levels of three candidate genes in the BSR population pools.

Figure S6 Digital expression patterns of the genes located within the 134.0–135.9 Mb (CS V1.0) loci of chromosome 7AS.

Figure S7 Digital expression patterns of three *TaTPP* homologues in different tissues and at various developmental stages of CS.

Figure S8 Agronomic traits of transgenic lines and WT plants in the field.

Figure S9 Phenotype of the harvested whole plants and spikes of the transgenic lines and WT plants.

Figure S10 Developing grain traits of transgenic lines and WT plants.

Figure S11 Lemma and palea phenotype of transgenic lines and WT plants.

Figure S12 PCR and sequencing-based identification of the *CriTaTPP* mutants.

Figure S13 Sequencing identification and phenotype evaluation of the *K-TaTPP* mutants.

Figure S14 Heatmap of genes of the grain size regulation clade (S14-1), photosynthesis and energy metabolism clade (14–2), and cell wall metabolism clade (14–3) in the transgenic OE lines and WT plants.

Figure S15 Decade frequency evolution analysis of the three haplotypes of *TaTPP-7A* during Chinese breeding.

Figure S16 Distribution of the three haplotypes of *TaTPP-7A* in 348 modern Chinese varieties.

Figure S17 Genomic polymorphism diagram based on *TaTPP-7A* resequencing in 47 accessions (six diploids, seven tetraploids, and 34 hexaploids).

Figure S18 TKW distribution diagram of the F_2 segregation progeny used in BSR-seq.

Table S1 *P*-values of the peaked SNPs at the GWAS loci (127.66–127.91 Mb) and the pairwise LD correlation coefficient in the LD window pin for the plot.

Table S2 Primers used in wheat *TaTPP-7A* nulli-tetrasome localization.

Table S3 Thermal properties (S3-1), viscosity (S3-2), and chain length distribution (3–3) in the starch granules of transgenic lines and WT plants.

Table S4 Agronomic trait association analysis of the three haplotypes of *TaTPP-7A* in Chinese 262 MCC.

Table S5 TKW and other agronomic traits of 716 F_2 segregation progeny used in BSR-seq.

Table S6 Agronomic traits and yield data of transgenic lines and WT plants in the field.

Table S7 Primers used to construct and confirm the transgenic OE lines, RNAi lines, and the *CriTaTPP* and *K-TaTPP* mutants.

Table S8 Primers used to analyse the expression of *TaTPPs*.

Table S9 Statistics of clean reads from BSR-seq and RNA-seq.

Table S10 Heatmap data of the *TaTPP-7A* OE lines and WT plants used in RNA-seq.

Table S11 Accession numbers of genes used for phylogenetic analysis.

Table S12 Primers used to amplify the genomic, cDNA, and promoter sequences of *TaTPPs*.

Table S13 KASP primers used in genotyping *TaTPP-7A* haplotypes.

© 2023 The Authors. *Plant Biotechnology Journal* published by Society for Experimental Biology and The Association of Applied Biologists and John Wiley & Sons Ltd., 1–17

14677652, 0, Downloaded from https://onlinelibrary.wiley.com/doi/10.1111/pbi.14025 by Chinese Academy Of, Wiley Online Library on [15/03/2023]. See the Terms and Conditions (https://onlinelibrary.wiley.com/terms-and-conditions) on Wiley Online Library for rules of use; OA articles are governed by the applicable Creative Commons License